Bioorg. Med. Chem. 95 (2023) 117499

Contents lists available at ScienceDirect

Bioorganic & Medicinal Chemistry

journal homepage: www.elsevier.com/locate/bmc

# A novel genetically-encoded bicyclic peptide inhibitor of human urokinase-type plasminogen activator with better cross-reactivity toward the murine orthologue

Ylenia Mazzocato [a], Stefano Perin [a], Julia Morales-Sanfrutos [b], Zhanna Romanyuk [a], Stefano Pluda [a,c], Laura Acquasaliente [d], Giuseppe Borsato [a], Vincenzo De Filippis [d], Alessandro Scarso [a], Alessandro Angelini [a,e,*]

[a] Department of Molecular Sciences and Nanosystems, Ca' Foscari University of Venice, Via Torino 155, 30172 Venice, Italy
[b] Proteomics Unit, Spanish National Cancer Research Centre (CNIO), C. de Melchor Fernández Almagro 3, 28029 Madrid, Spain
[c] Fidia Farmaceutici S.p.A., Via Ponte della Fabbrica 3/A, Abano Terme 35031, Italy
[d] Department of Pharmaceutical and Pharmacological Sciences, School of Medicine, University of Padova, Via Marzolo 5, 35131 Padova, Italy
[e] European Centre for Living Technology (ECLT), Ca' Bottacin, Dorsoduro 3911, Calle Crosera, 30123 Venice, Italy

ARTICLE INFO

*Keywords:*
Phage display
Directed evolution
Affinity maturation
Cyclic peptide
Macrocycle
Urokinase-type plasminogen activator
uPA

ABSTRACT

The inhibition of human urokinase-type plasminogen activator (huPA), a serine protease that plays an important role in pericellular proteolysis, is a promising strategy to decrease the invasive and metastatic activity of tumour cells. However, the generation of selective small molecule huPA inhibitors has proven to be challenging due to the high structural similarity of huPA to other paralogue serine proteases. Efforts to generate more specific therapies have led to the development of cyclic peptide-based inhibitors with much higher selectivity against huPA. While this latter property is desired, the sparing of the orthologue murine poses difficulties for the testing of the inhibitor in preclinical mouse model. In this work, we have applied a Darwinian evolution-based approach to identify phage-encoded bicyclic peptide inhibitors of huPA with better cross-reactivity towards murine uPA (muPA). The best selected bicyclic peptide (UK132) inhibited huPA and muPA with $K_i$ values of 0.33 and 12.58 μM, respectively. The inhibition appears to be specific for uPA, as UK132 only weakly inhibits a panel of structurally similar serine proteases. Removal or substitution of the second loop with one not evolved *in vitro* led to monocyclic and bicyclic peptide analogues with lower potency than UK132. Moreover, swapping of 1,3,5-*tris*-(bromomethyl)-benzene with different small molecules not used in the phage selection, resulted in an 80-fold reduction of potency, revealing the important structural role of the branched cyclization linker. Further substitution of an arginine in UK132 to a lysine resulted in a bicyclic peptide UK140 with enhanced inhibitory potency against both huPA ($K_i = 0.20$ μM) and murine orthologue ($K_i = 2.79$ μM). By combining good specificity, nanomolar affinity and a low molecular mass, the bicyclic peptide inhibitor developed in this work may provide a novel human and murine cross-reactive lead for the development of a potent and selective anti-metastatic therapy.

## 1. Introduction

Human urokinase-type plasminogen activator (huPA) is a secreted trypsin-like serine protease involved in various physiological processes, such as extracellular matrix homeostasis and tissue remodelling.[1] Altered expression pattern of huPA has been associated with tumour growth, invasion, metastatic spread, and correlates with poor prognosis of cancer patients.[2] Hence, huPA represents a diagnostic, prognostic, and therapeutic target to reduce cancer-associated morbidity and mortality.[3]

Inhibition of huPA has been attempted by using various small molecule inhibitors, among which only a limited number was tested in clinical trials.[4,5] The most advanced huPA inhibitor is WX-671 ($K_i = 0.9$ μM)[6], an orally administered 3-aminophenylalanine pro-drug

* Corresponding author at: Prof. Dr. Alessandro Angelini, Department of Molecular Sciences and Nanosystems, Ca' Foscari University of Venice, Via Torino 155, 30172 Venice, Italy.
*E-mail address:* alessandro.angelini@unive.it (A. Angelini).

https://doi.org/10.1016/j.bmc.2023.117499
Received 25 March 2023; Received in revised form 30 August 2023; Accepted 10 October 2023
Available online 12 October 2023

derivative, also known as Upamostat or Mesupron®.[7] WX-671 showed potential antineoplastic and antimetastatic activities in preclinical studies and has completed two phase II proof of concept clinical studies suggesting activity as measured by both tumour response rate and overall survival of patients when administered in combination with first-line chemotherapeutic agents.[8–12] However, recent studies have revealed that WX-671 has low specificity and also inhibits a panel of other related human trypsin-like serine proteases such as tissue-type plasminogen activator (tPA; $K_i$ = 1.4 μM), plasmin ($K_i$ = 2.4 μM), thrombin ($K_i$ = 0.8 μM), matriptase ($K_i$ = 0.20 μM) and multiple trypsin members ($K_i$ = 0.019 – 0.19 μM).[6,13–15] The high specificity is crucial for therapeutic use, since several of these closely related enzymes play important roles in blood-clotting, fibrinolysis, immunity or other physiological functions, and they should not be blocked by huPA inhibitors.

Efforts to generate more effective and specific therapies have led to the development of peptide-based inhibitors.[16,17] Unlike small molecule-based inhibitors, peptides often display a higher selectivity as a result of increased interaction interface between the protease and the inhibitor and the ability to also contact distant residues present in less conserved subsites of huPA.[18,19] Toward this goal, a series of potent and selective huPA inhibitors were developed based on amidinobenzylamine peptidomimetics.[20] One compound from the latter group, CJ-463 (benzylsulfonyl-D-Ser-Ser-4-amidinobenzylamide; $K_i$ = 20 nM), has shown to reduce primary tumour growth and metastasis formation in a murine lung carcinoma model.[20–23] Though CJ-463 was much more selective than the first generation of small-molecular-weight huPA inhibitors and did not significantly inhibit a range of human relevant proteases (tPA, thrombin, factor Xa, plasma kallikrein), the compound showed weak inhibition of plasmin ($K_i$ = 0.75 μM) and strong inhibition of trypsin ($K_i$ = 22 nM).[20–23]

With the aim of generating more potent and selective peptide-based huPA inhibitors, we and other research groups used cyclic peptides and applied phage-display based approaches to screen large combinatorial libraries of cyclic peptides.[18,24,25] Compared to linear analogues, cyclic peptides display reduced conformational freedom that can limit the entropic penalty upon binding to a target, leading to a higher binding affinity.[25] Notably, the reduced flexibility typically also makes cyclic peptides less susceptible to metabolic degradation compared to their linear analogues.[26,27] Phage-encoded monocyclic peptide inhibitors of huPA have been previously developed by the group of Andreasen P. A. who isolated a highly selective disulfide cyclised inhibitor (upain-1, CSWRGLENHRMC) with a $K_i$ value of 29.9 μM.[28,29] Further affinity maturation experiments led to the discovery of a peptide variant (DGACSWRGLENHAAC) with ~6-fold higher potency ($K_i$ = 4.6 μM).[30] The same group also succeeded in generating murine uPA (muPA) specific peptide-based inhibitors capable of suppressing tumour growth and cancer metastasis in tumour-bearing mice.[31,32] We therefore reasoned that it should be possible to obtain huPA inhibitors with even higher affinities by using bicyclic peptides.[33] Bicyclic peptides contain two connected macrocyclic rings that can both engage in binding with the protease. Compared to monocyclic analogues of comparable size, bicyclic peptides are less flexible.[25] Structurally diverse genetically encoded bicyclic peptide inhibitors of huPA were isolated from large combinatorial repertoire of phage-display peptide library containing three cysteine residues that prior to affinity selection have been cyclized either by oxidation of cysteines or by alkylation upon reaction with small organochemical scaffolds.[24,34–37] The most potent phage-encoded bicyclic peptide selected against huPA was UK18 (ACSRYEVDCRGRGSACG), a 1,3,5-*tris*-(bromomethyl)-benzene (TBMB) modified bicycle peptide with a $K_i$ value of 53 nM.[24] Importantly, inhibition appears to be highly specific to huPA, as the peptide only weakly inhibits a panel of related human and murine serine proteases ($K_i$'s > 100 μM).[24] Attempts to affinity mature UK18 by mutating amino acids around the conserved region did not yield more potent inhibitors.[24] However, moderate improvement in inhibitory activity ($K_i$ = 28 nM) and plasma stability (4-fold) were observed when a L-glycine residue, that has a positive dihedral angle when bound to the target, was replaced by a D-serine.[38] Despite a high potency and exquisite specificity, bicyclic peptide inhibitor UK18 failed to significantly reduce the growth rate of human xenograft tumours in immunocompromised mice model.[39] This result raised the question of whether tumour growth depends not only on huPA produced by the primary tumour but also on orthologue muPA secreted by the host surrounding stroma. Indeed, activity of uPA derived from stromal cells is well known to play crucial roles in tumour development and metastasis.[40] This hypothesis is further supported by a recent study reporting a muPA-specific monocyclic peptide-based inhibitor capable of significantly suppressing tumour growth and cancer metastases in a syngeneic tumour mouse model.[32]

In the present study, we undertook a new attempt to isolate novel phage-encoded bicyclic peptide inhibitors of huPA with better cross-reactivity towards muPA by affinity maturing a different consensus motif present in several bicyclic peptides that were identified in previous phage selection campaigns using diverse naïve peptide libraries.[24,34–37] The best affinity matured bicyclic peptide inhibited both huPA and muPA, though the latter at low micromolar concentrations. Removal or substitution of the second loop with one not evolved *in vitro* led to monocyclic and bicyclic peptide analogues with lower potency, thus underlining the importance of the second loop. Further studies revealed that both constrains of the peptide and the nature of the central branched cyclisation linker are key for potency of inhibition. Finally, site-specific substitution of an arginine with a lysine led to a peptide variant with even higher inhibitory potency against both huPA and muPA while retaining specificity towards numerous others serine proteases.

## 2. Results

### 2.1. Affinity maturation yielded bicyclic peptide inhibitors of huPA with enhanced potency over parental clones

To improve the potency of previously identified clones that shared a strong consensus motif ($^{R}/_{K}^{F}/_{Y}^{S}/_{T}$) and had inhibitory activities in the micromolar range (**Supplementary figure 1**), we generated a novel combinatorial phage-display peptide library of structurally diverse bicyclic peptides fused to the disulfide-free gene-3-protein (g3p). The phage-display peptide library was designed in the format $CX_nCX_nC$ ($n$ = 6; X = any amino acid) and comprised $2.0 \times 10^8$ different peptide sequences. Amino acid residues belonging to the highly conserved consensus motif in the first peptide loop, potentially playing an important role in binding, were partially altered while the six amino acids of the second loop were completely randomized (library: $ACN^{A}/_{S}R$-$^{F}/_{Y}^{S}/_{T}GCXXXXXXCG$; **Figure 1**a). Since most of the huPA peptide-based inhibitors developed so far include an arginine capable of interacting tightly with the aspartic acid present at the bottom of the S1 pocket, the arginine at position 5 was kept fixed. Moreover, the presence of an arginine instead of a lysine excluded the presence of free reactive primary amines that could hinder further selective bioconjugation processes.

The phage-display peptide library was reacted with the three thiol-reactive small organic molecule TBMB to obtain a repertoire of phage-encoded bicyclic peptide structures and panned against huPA. To promote the selection of clones displaying increased binding affinity toward huPA we allowed the mutants to evolve through three sequential rounds of equilibrium-based selection using decreasing concentrations of biotinylated huPA (280 – 1.42 pmol). Streptavidin and neutravidin magnetic beads were alternated to avoid enrichments of potential streptavidin or neutravidin binders. Already in the first round of selection, the number of phage particles isolated against huPA was 100-fold higher compared to the negative control selection. The enrichment over the negative control rose to 10000-fold in the third round. Subsequent Sanger sequencing of selected clones revealed the presence of thirty-seven unique peptide sequences (**Figure 1a**).

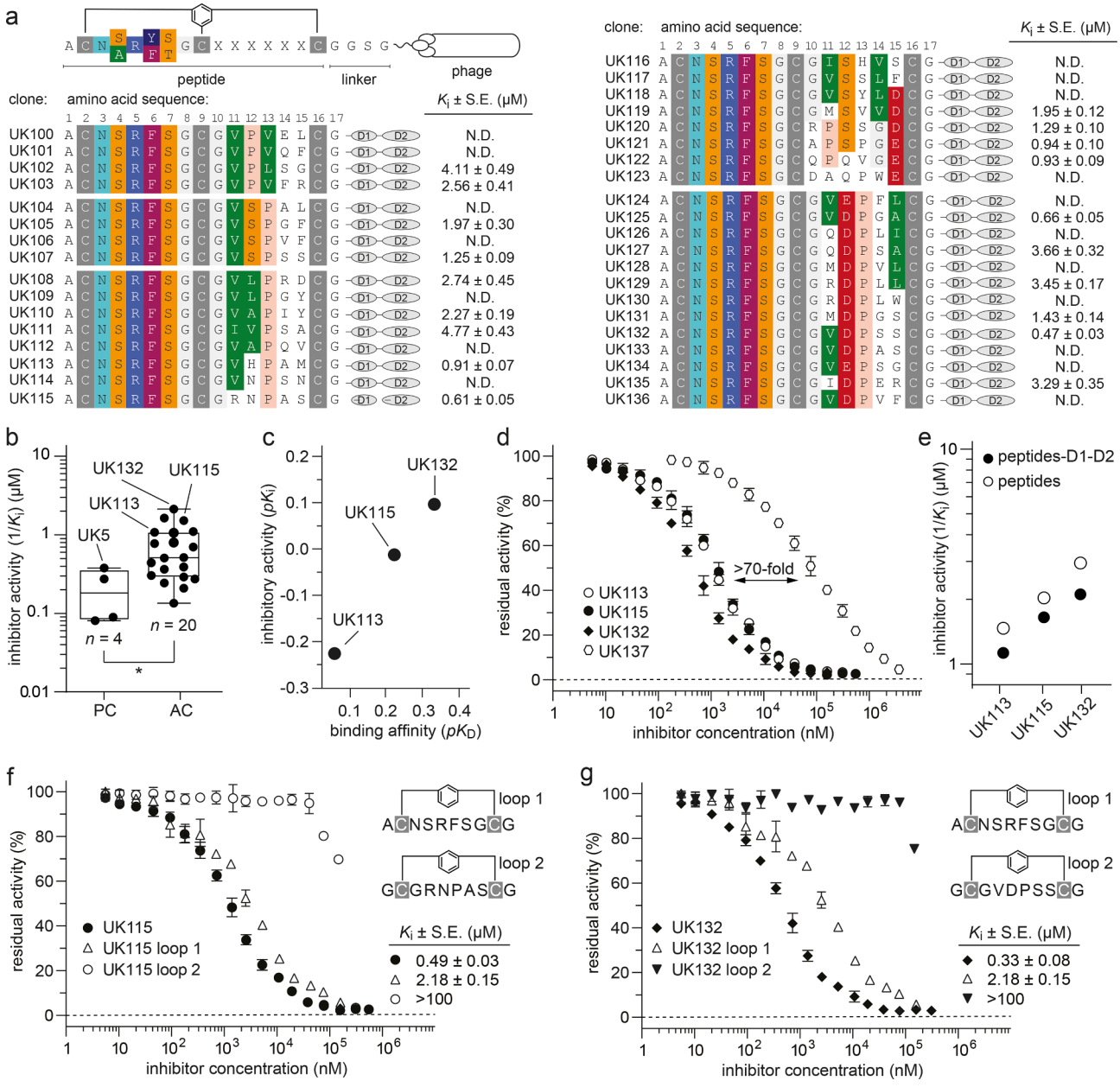


**Figure 1. Phage selected affinity matured bicyclic peptides against huPA. a**) Top left, the design of the phage-display peptide library is shown. Bottom and right, sequences of selected clones from a semi randomised peptide library are shown. The sequences are arranged in groups according to sequence similarities. Identical or similar amino acids between different peptide sequences are highlighted in colour. The inhibitory activities ($K_i$s) of nineteen TBMB-cyclised peptides (as D1-D2 fusion peptides) were determined at 25 °C and physiological pH (7.4) using the suitable substrate at a concentration of 50 μM. Mean values of at least three measurements are indicated. S.E., standard error; N.D., not determined; **b**) Box-and-whiskers plot comparing the $K_i$ values determined for the parental clones (PC, left) and the affinity matured one (AC, right), "*n*" indicates sample size. Statistical comparisons were performed between each group using one-way analysis of variance (ANOVA), followed by Tukey's test to calculate *P*-values (*$P < 0.05$); **c**) Plot displaying the inhibitory activity ($pK_i$) versus the binding affinity ($pK_D$) of UK113, UK115 and UK132 bicyclic peptide fusions; **d**) Residual activities of huPA incubated with synthetic bicyclic peptides UK113, UK115, UK132 and UK137; **e**) Plot displaying the $K_i$ values (means) of UK113, UK115 and UK132 determined in the format of synthetic (black dots) or recombinant fusion (white dots) bicyclic peptide inhibitors; **f**) Residual activities of huPA incubated with synthetic bicyclic peptide UK115 and its derived individual peptide rings (UK115-loop 1 and UK115-loop 2) modified with 1,3-*bis*-(bromomethyl)-benzene; **g**) Residual activities of huPA incubated with synthetic bicyclic peptide UK132 and its derived individual peptide rings (UK132-loop 1 and UK132-loop 2) modified with 1,3-*bis*-(bromomethyl)-benzene.

A comparison of the isolated bicyclic peptides showed a strong convergent evolution of amino acids in the first loop with a preference of serine (S) over alanine (A) in position 4, phenylalanine (F) over tyrosine (Y) in position 6 and serine (S) over threonine (T) in position 7. In addition, almost all selected clones showed a glycine (G) in position 10, a strong enrichment of hydrophobic branched residues such as valine (V) and leucine (L) in position 11, a proline (P) either in position 12 or 13, and a negatively charged residue (D or E) in position 15 (Figure 1**a**).

Next, nineteen of the identified bicyclic peptides were recombinantly produced as fusions to the cysteine-free *N*-terminal domains (D1 and D2) of the phage protein 3 (g3p),[24] purified and post-translationally cyclized with TBMB (Supplementary figure 2 and supplementary table 2). Furthermore, their inhibitory activities were determined by measuring the residual activity of huPA with a fluorogenic substrate at physiological pH (7.4) and room temperature (25 °C). Most of the bicyclic peptide fusion proteins showed improved potency over the parental clones with

$K_i$ values in the high nanomolar and low micromolar range (Figure 1**a, b**). The three best polypeptide-TBMB conjugates (UK113, UK115 and UK132) showed $K_i$ values ranging from 0.47 to 0.91 μM (Figure 1**a**).

Then, we assessed the binding affinities of the three UK113, UK115 and UK132 bicyclic peptide fusions to huPA by surface plasmon resonance (Supplementary figure 3). Remarkably, the determined binding constant ($K_D$) values, ranging from 0.80 to 1.70 μM (Table 1), correlated well with the $K_i$ values (Figure 1**c**).

The three peptides were then chemically synthesised by solid-phase peptide synthesis. Reaction with TBMB yielded single products with a molecular mass corresponding to the desired products (Supplementary figure 4 and Supplementary table 3). Chemically synthesised bicyclic peptides UK113, UK115 and UK132 showed $K_i$ values of 0.69, 0.49 and 0.33 μM, respectively (Figure 1**d** and Table 2). The inhibitory potency of all three synthetic bicyclic peptides is higher than that of the same molecules tested as bicyclic peptide-D1-D2 fusion proteins (Figure 1**e**).

To assess the contribution of the affinity matured second peptide loop, we synthesised a bicyclic peptide analogue, named UK137, in which the amino acid residues of the second loop were replaced by a glycine and serine linker (GSGSGS), while those of the first loop were kept identical to that of UK113, UK115 and UK132. Notably, bicyclic peptide UK137 inhibited huPA with a $K_i$ of 51.39 μM which is approximately 155-fold higher than that of UK132 (Figure 1**d** and Table 2).

To pinpoint the contribution of each single peptide loop, we synthesised monocyclic peptide analogues of UK115 and UK132, the two most potent affinity matured inhibitors. Single macrocyclic rings were generated by connecting the two terminal cysteines of each peptide loop with 1,3-*bis*-(bromomethyl)-benzene (DBMB; Supplementary figure 5 and Supplementary table 3 and 4). Notably, the first loop of UK115 (identical to that of UK132) crosslinked with DBMB inhibited huPA with a $K_i$ value of 2.18 μM, around 4- and 6-fold weaker than that of the bicyclic peptide UK115 ($K_i$ = 0.49 μM) and UK132 ($K_i$ = 0.33 μM), respectively (Figure 1**f**,**g**). In contrast, the second loop of UK115 and UK132 crosslinked with DBMB inhibited huPA with very low potency ($K_i$ >100 μM).

Overall, the affinity maturation effort yielded a range of bicyclic peptide inhibitors with at least 4-fold improved potency over the parental clones. Although the bicyclic modality showed higher potency, a single loop appears to play a major contribution in inhibiting huPA.

### 2.2. Bicyclic peptide UK132 recognises both human and murine uPA

To assess the specificity of UK132, we determined its inhibitory constants ($K_i$s) against a panel of structurally and functionally related human and murine trypsin-like proteases. Human and murine tPA (htPA and mtPA), two homologue serine proteases that share with uPA the same primary physiological substrate and inhibitors, were only weakly inhibited ($K_i$ >300 μM; Figure 2). Bicyclic peptide UK132 revealed >1000-fold selectivity ($K_i$ >300 μM) over other human serine proteases, such as thrombin, plasmin, plasma kallikrein and factor XIIa, which share high sequence identities with huPA (Figure 2). The only exception was human trypsin, which showed a $K_i$ value of 90.28 μM, around 270-fold higher than that measured for huPA. Notably, murine uPA (muPA; 71% sequence identity with huPA) was inhibited with a $K_i$ value of 12.58 μM, about 38-fold higher than that determined for huPA (Figure 2). Taken together, these data indicate that bicyclic peptide UK132 appears to cross-react with both huPA and muPA, and only weakly inhibits a panel of related serine proteases.

**Table 1**
**Binding affinity of the best bicyclic peptide fusion proteins.** Binding kinetics of three selected bicyclic peptide-D1-D2 fusion proteins modified with TBMB (UK113, UK115 and UK132) toward immobilised huPA were determined by surface plasmon resonance at 25 °C and physiological pH (7.4). S.E., standard error.

| Binding affinity | | | |
|---|---|---|---|
| **Clone** | **$k_{on}$ ± S.E. ($M^{-1}·s^{-1}$)** | **$k_{off}$ ± S.E. ($s^{-1}$)** | **$K_D$ ± S.E. (M)** |
| UK113-D1-D2 | $(3.4 \pm 1.6) \times 10^4$ | $(3.1 \pm 1.5) \times 10^{-2}$ | $(1.70 \pm 0.68) \times 10^{-6}$ |
| UK115-D1-D2 | $(4.3 \pm 2.3) \times 10^4$ | $(2.32 \pm 0.98) \times 10^{-2}$ | $(1.03 \pm 0.52) \times 10^{-6}$ |
| UK132-D1-D2 | $(4.3 \pm 2.5) \times 10^4$ | $(2.2 \pm 1.0) \times 10^{-2}$ | $(0.80 \pm 0.49) \times 10^{-6}$ |

**Table 2**
**Inhibitory activity of synthetic bicyclic peptides**. The inhibitory activity ($K_i$) values of four synthetic bicyclic peptides (UK113, UK115, UK132 and UK137) towards huPA protease were determined at 25 °C and physiological pH (7.4) using the suitable substrate at a concentration of 50 μM. The $K_m$ value of huPA protease was determined by standard Michaelis-Menten kinetics and used in the calculation of the reported $K_i$ values. The shown values are the means of three independent experiments. S.E., standard error. C-terminus is amidated.

| Inhibitory activity of bicyclic peptides | | |
|---|---|---|
| **Clone** | **peptide amino acid sequence** | **$K_i$ ± S.E. (μM)** |
| UK113 | H-ACNSRFSGCGVHPAMCG-$NH_2$ | 0.69 ± 0.03 |
| UK115 | H-ACNSRFSGCGRNPASCG-$NH_2$ | 0.49 ± 0.03 |
| UK132 | H-ACNSRFSGCGVDPSSCG-$NH_2$ | 0.33 ± 0.01 |
| UK137 | H-ACNSRFSGCGSGSGSCG-$NH_2$ | 51.39 ± 0.70 |

### 2.3. The inhibitory potency of UK132 is determined by backbone conformational preferences

To assess the contribution of the backbone conformational rigidity to the inhibitory potency of UK132 against huPA, we synthesised a linear and a monocyclic analogue of the bicyclic peptide and compared their activities. The linear variant, named UK132$^{SSS}$, has serine residues instead of cysteines in the three amino acid positions 2, 9 and 16 to disable oxidative cyclisation (H-ASNSRFSGSGVDPSSSG-NH2) (Figure 3**a** and Supplementary Figure 5). This linear peptide analogue inhibited huPA with low potency ($K_i$ = 199.50 μM) (Figure 3**b**). Another variant, named UK132$^{CSC}$, was synthesised with a single serine residue and two cysteines (H-ACNSRFSGSGVDPSSCG-NH2) and crosslinked with DBMB (Figure 3**a** and Supplementary Figure 5). This monocyclic peptide inhibited huPA with a $K_i$ of 30.40 μM intermediate between those of the linear and the bicyclic peptides (Figure 3**b**). In summary, the inhibition of the linear and the monocyclic analogues was around 600- and 90-fold weaker than that of the bicyclic peptide UK132, respectively. These data showed that increasing conformational constrains of the peptide led to improved inhibitory potency.

To evaluate the role of the small central hydrophobic linker TBMB on the conformation of the peptide backbone, the linear peptide UK132 containing three cysteine moieties was cyclised with two different chemical linkers and their activities were assessed. The two synthetic linkers, namely 2,4,6-*tris*-(bromomethyl)-mesitylene (TBMM) and 1,3,5-*tris*-(bromomethyl)-2,4,6-triethylbenzene (TBME), comprise additional groups at positions 2, 4 and 6 of the aromatic rings that could provide different environments and hence affect the conformation of the bicyclic peptide as well as its potency of inhibition (Figure 3**c**). UK132 peptide cyclised with TBMM (UK132-TBMM) or with TBME (UK132-TBME) inhibited huPA approximately 80- and 138-fold weaker ($K_i$ values of 26.45 μM and 45.74 μM, respectively) than UK132-TBMB (Figure 3**d** and Supplementary Figure 5). Overall, the swapping experiment confirmed that the peptide had adapted to the structural and chemical environment of the small hydrophobic molecule. The large variations in $K_i$ values obtained using the same peptide sequence modified with different chemical linkers underlined not only the importance of the bicyclic configuration but also the key role played by the type of small organic linker used for the phage selection.

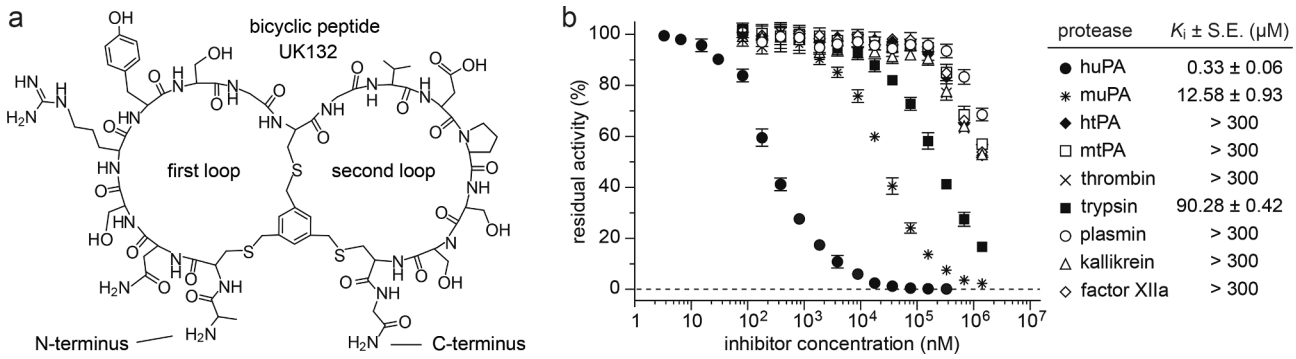


**Figure 2. Specificity of synthetic bicyclic peptide UK132.** **a**) Chemical structure of bicyclic peptide UK132; **b**) Residual activities of huPA and a series of homologous human and murine trypsin-like serine proteases incubated with synthetic bicyclic peptide UK132 were determined at 25 °C, at physiological pH (7.4) using the suitable substrates at a concentration of 50 μM. The shown values are the means of three independent experiments. Data are presented as mean (symbol). S.E., standard error. The $K_m$ values of each protease were determined by standard Michaelis-Menten kinetics and used in the calculation of the reported $K_i$ values (Supplementary table 1).

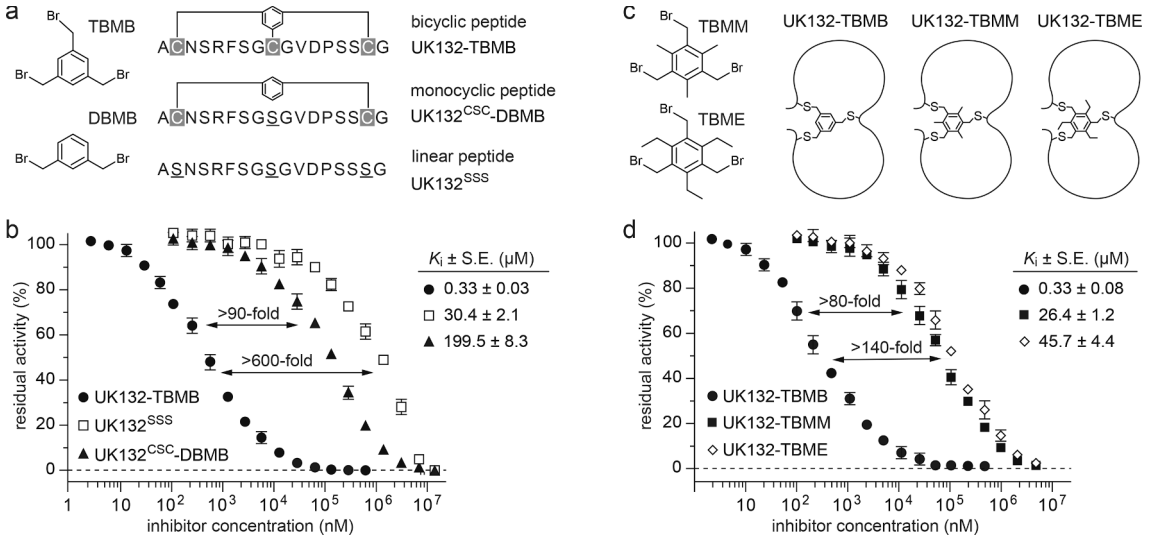


**Figure 3. Role of cyclisation and small central hydrophobic linker in the inhibitory activity of UK132.** **a**) Schematic depiction of UK132 bicyclic (top), monocyclic (middle) and linear (bottom) peptide variants. Monocyclic derivative UK132$^{CSC}$-DBMB was obtained by replacing the middle cysteine with a serine and the flanking cysteines reacted with DBMB. Linear derivative UK132$^{SSS}$ was obtained by replacing the three cysteine residues with serine; **b**) Residual activities of huPA incubated with linear (UK132$^{SSS}$), monocyclic (UK132$^{CSC}$-DBMB) and bicyclic (UK132-TBMB) peptides. The shown values are the means of three independent experiments. Data are presented as mean (symbol). S.E., standard error; **c**) Schematic depiction of the bicyclic peptide UK132 modified with TBMB (left), TBMM (middle) and TBME (right) cross-linking agents; **d**) Residual activities of huPA measured at different concentrations of UK132-TBMB, UK132-TBMM and UK132-TBME bicyclic peptides. The shown values are the means of three independent experiments. Data are presented as mean (symbol). S.E., standard error. The inhibitory activities of all peptide variants towards huPA were determined at 25 °C and physiological pH (7.4) using the suitable substrate at a concentration of 50 μM. The $K_m$ value of huPA protease was determined by standard Michaelis-Menten kinetics and used in the calculation of the reported $K_i$ values. S.E., standard error.

### *2.4. Substitution of an arginine to a lysine resulted in a bicycle peptide with enhanced inhibitory potency against human and murine uPA*

To confirm that the enriched residues serine and phenylalanine in position 4 and 6 of the consensus motif ($^{R}/_{K}^{F}/_{Y}^{S}/_{T}$) present in the first loop, respectively, are the result of a convergent evolution, we generated two bicyclic peptide variants in which the serine was replaced by an alanine (S → A; UK138) and the phenylalanine by a tyrosine (F → Y; UK139; Supplementary Figure 6). Both UK138 and UK139 variants inhibited huPA with $K_i$ values of 2156 and 1404 nM, approximately 6- and 4-fold weaker than the phage-selected bicyclic peptide UK132 (Figure 4). Next, we questioned whether it was worth preferring arginine to lysine in position 5. Surprisingly, bicyclic peptide UK140 with lysine instead of arginine (R → K) showed a $K_i$ value of 202 nM, around 1.6-fold better than UK132 (Figure 4). Additionally, we combined the mutations together to investigate the possibility of even further higher potency. Bicyclic peptide UK141, sharing an alanine in position 4 and a lysine in position 5, displayed a $K_i$ value of 484 nM while UK142, that includes a lysine in position 5 and a tyrosine in position 6, showed a $K_i$ of 359 nM (Figure 4).

Taken together, these data indicate that the residues serine in position 4 and phenylalanine in position 6 are critical, as attempts to revert them to their alternative amino acid resulted in bicyclic peptides with lower potency, suggesting a convergent selection pressure for these two residues. The only exception appears to be represented by position 5, in which mutation of the arginine, that was kept unaltered during the selection, to a lysine resulted in UK140, a bicycle peptide with enhanced inhibitory potency against huPA.

To confirm the selectivity of the new peptide variant UK140, we determined its inhibitory constants ($K_i$s) against a panel of structurally and functionally related human and murine trypsin-like proteases. While bicyclic peptide UK140 retained >1000-fold selectivity ($K_i$ >300 μM) over human tPA, murine tPA, human thrombin, human plasmin, human plasma kallikrein, human factor VIIa, Xa, XIa, XIIa and human

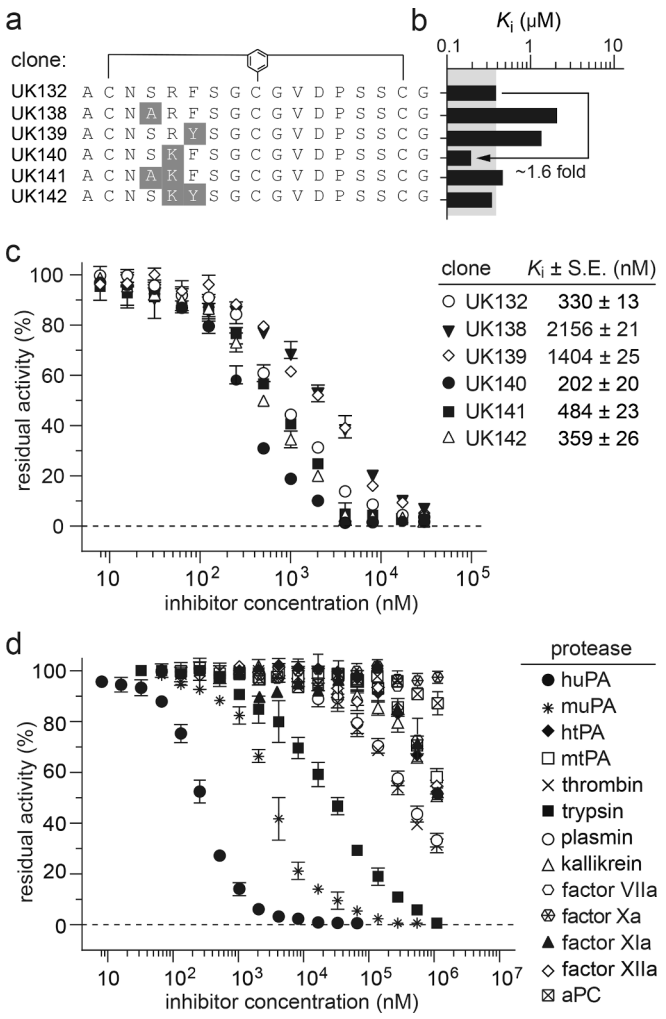


**Figure 4. Identification and characterisation of bicyclic peptide variant UK140.** **a**) Amino acid sequences of five different UK132-derived bicyclic peptide variants (UK138 – UK142). Mutated residues are highlighted in grey; **b**) Column graph comparing the determined $K_i$ values for UK132 and five mutated variants (UK138 – UK142); **c**) Residual activities of huPA measured at different concentrations of bicyclic peptide variants. The shown values are the means of three independent experiments. Data are presented as mean (symbol). The inhibitory activities of all peptide variants towards huPA protease were determined at 25 °C and physiological pH (7.4) using the suitable substrate at a concentration of 50 μM. The $K_m$ value of huPA protease was determined by standard Michaelis-Menten kinetics and used in the calculation of the reported $K_i$ values. S.E., standard error; **d**) Residual activities of huPA and a series of homologous human and murine trypsin-like serine proteases incubated with synthetic bicyclic peptide UK140 were determined at 25 °C, at physiological pH (7.4) using the suitable substrates at a concentration of 50 μM for human and murine uPA, human and murine tPA, human thrombin, human trypsin, human kallikrein and human factor XIIa and at a concentration of 200 μM for human factor VIIa, Xa and XIa, and human activated protein C (aPC). The shown values are the means of three independent experiments. Data are presented as mean (symbol). S.E., standard error.

activated protein C (aPC), it inhibited human trypsin with a $K_i$ value of 10.52 μM, around 8.5-fold better than that determined for UK132 (Figure 4 and Table 3). However, an increase in inhibitory potency of UK140 has been also observed when tested against muPA ($K_i$ = 2.79 μM), around 4.5-fold better than that determined for UK132 (Figure 4 and Table 3). Taken together, these data indicate that bicyclic peptide UK140 can inhibit both huPA and muPA, though the latter with $K_i$ values in the low micromolar range.

Likewise UK132, single macrocyclic rings generated by connecting

**Table 3**
**Specificity of synthetic bicyclic peptide UK140.** The inhibitory activity ($K_i$) values of synthetic bicyclic peptide UK140 towards multiple human and murine serine proteases were determined at 25 °C and physiological pH (7.4) using the suitable substrate at a concentration of 50 μM for human and murine uPA, human and murine tPA, human thrombin, human trypsin, human kallikrein and human factor XIIa and at a concentration of 200 μM for human factor VIIa, Xa and XIa, and human activated protein C. The $K_m$ values of each protease were determined by standard Michaelis-Menten kinetics (Supplementary table 1) and used in the calculation of the reported $K_i$ values. The shown values are the means of three independent experiments. S.E., standard error. C-terminus is amidated.

| Specificity of bicyclic peptide UK140 | |
|---|---|
| **Serine protease** | **$K_i$ ± S.E. (μM)** |
| human uPA | 0.20 ± 0.02 |
| murine uPA | 2.79 ± 0.32 |
| human tPA | > 300 |
| murine tPA | > 300 |
| human thrombin | > 300 |
| human trypsin | 10.52 ± 0.12 |
| human plasmin | > 300 |
| human kallikrein | > 300 |
| human factor VIIa | > 300 |
| human factor Xa | > 300 |
| human factor XIa | > 300 |
| human factor XIIa | > 300 |
| human activated protein C | > 300 |

the two terminal cysteines of each peptide loop of UK140 with DBMB (Supplementary figure 5 and Supplementary table 3 and 4) inhibited huPA with a $K_i$ value of 4.58 μM (first loop) and >100 μM (second loop), around 22– and >500-fold weaker than that of the bicyclic peptide UK140, respectively (Supplementary figure 8). This data further underlines the role of the second loop.

## 3. Discussion and conclusions

Human urokinase-type plasminogen activator (uPA) contributes to a wide range of physiological processes and its aberrant expression or dysregulated activity has been linked to the development of different diseases such as cancer and rheumatoid arthritis, to name but few. Hence, huPA represents an important drug target for the treatment of several human pathologies.[41]

Inhibition of huPA has been attempted using various small molecules. However, conventional small molecule-based inhibitors have had limited success in the clinic. Failures have often been attributed to off-target effects due to structural similarities between the active sites of the numerous (>70) physiologically relevant trypsin-like serine proteases present in humans. For example, the highly related human proteases tPA, plasmin, trypsin and plasma kallikrein have 45, 37, 37 and 33% of identical amino acids respectively, and the sequence identity within 4.5 Å distance of the active site in all these members is higher than 72%.[42]

Efforts to generate more effective therapies have led to the development of peptide-based inhibitors. Unlike small molecules, peptide-based inhibitors can bind to the target with a larger surface of interaction to obtain high affinity and recognise surface-exposed loops that are less conserved among closely related serine proteases to enable higher selectivity. Although the latter property is desired, the high specificity towards the solely human enzyme poses difficulties for testing the inhibitors in preclinical animal models. Indeed, previously developed bicyclic peptides with exquisite specificity towards huPA failed to significantly reduce the tumour growth rate in mice model,[39] probably because a key role in tumour development and metastasis is also played by the orthologue murine uPA (muPA) which is produced by the tumour-surrounding endogenous stromal cells and not effectively blocked by the peptide inhibitor.[32,40]

In this work, we applied a directed evolution-based approach to isolate novel phage-encoded bicyclic peptide inhibitors of huPA with better cross-reactivity towards muPA. Affinity maturation of a partially randomised combinatorial bicyclic peptide library bearing a consensus motif in the first peptide loop yielded novel post-translationally chemically modified peptides with consensus sequences also in the second peptide loop. Notably, the newly selected bicycle peptides do not share similarities with previously identified peptide-based huPA inhibitors and showed a strong convergent evolution of numerous amino acids present in both peptide loops. The most potent selected inhibitor (UK132) displayed an inhibitory activity of 330 nM, which is around 4-fold better than the best parental clone.[24] The inhibition of UK132 appears to be highly specific for huPA, as the peptide only weakly inhibits a panel of related human and murine trypsin-like serine proteases (>100-fold selectivity). The high specificity of UK132 for huPA was pleasing since many of the paralogous serine proteases tested have vital biological functions and their inhibition could cause severe side effects. Notably, among the different serine proteases tested, only the orthologue muPA was inhibited by UK132, though at a low micromolar concentration.

Further substitution of some key enriched residues localised in the first semi-randomised loop of UK132 allowed us to redefine the consensus motif and better appreciate the contribution of single amino acids to the binding. While the substitution of the phage-selected residues serine in position 4 and phenylalanine in position 6 to an alanine and a tyrosine, respectively, resulted in peptides whose potency was reduced by 6- and 4-fold, site-specific substitution of the left unaltered arginine in position 5 with a lysine led to the peptide variant UK140 with enhanced inhibitory potency and retained specificity. Although most of the substrates, as well as numerous endogenous and exogenous peptidic inhibitors of huPA described so far, have an arginine, that through the guanidinium group, engages in multiple contacts with the carboxyl group of the aspartic acid present in the highly conserved S1 pocket,[43–45] there are also examples of peptide-based inhibitors, such as the Kunitz-domain based inhibitors, in which P1 arginine present in the solvent-exposed loop is often replaced by a lysine that inserts well into the S1 site.[46]

The high affinity and specificity of both UK132 and UK140 bicyclic peptides can be ascribed to a complex balance of both entropic and enthalpic factors. Indeed, when bicyclic peptide UK132 was not or only partially cyclised, its activity dropped more than 90-fold, indicating that increasing conformational constrains of the backbone might have enabled the generation of molecules with lower entropic penalty and ultimately improved binding affinities. This hypothesis is in line with previous studies reporting that peptide cyclisation improves the rigidity leading to changes in entropy and enthalpy that might be favourable for the thermodynamic stability (e.g., formation of preorganized structures).[33,47–49] However, a reduction in conformational entropy penalty due to peptide cyclisation or pre-organization can be counterbalanced by an unfavourable vibrational entropy change if the constraints are too rigid.[50–52] For example, further constrain of a monocyclic peptide inhibitor had led to the development of a novel bicyclic peptide inhibitor with reduced binding entropic penalty, which, however, was partially offset by an increased enthalpy and only moderately enhanced inhibitory potency.[53] Furthermore, the role of water and the enthalpy/entropy compensation phenomenon associated to it must be also carefully considered.[54] These show that the entropic relationship between a bicyclic peptide ligand and its less constrained counterparts can be a complex one that is difficult to rationalise based on solely experimental binding affinities. Additional in solution studies using isothermal titration calorimetry (ITC) and nuclear magnetic resonance (NMR) spectroscopy will be needed to truly understand the delicate interplay between enthalpy and entropy of our cyclic and linear peptide forms.

Further swapping experiment performed to assess the role of the small hydrophobic linker TBMB on the conformation of the peptide backbone showed a reduction in potency of more than 80-fold, highlighting the key structural role of the branched cyclisation linker. The dominant effect of the small hydrophobic linker can be explained by its central positioning, forming the branching point of the bicyclic peptide. Addition of small chemical groups, such as methyl (TBMM) or ethyl (TBME) chains, appear to offer diverse environments to the peptides and hence, through either non-polar interactions or steric exclusion, perturb or impose novel and unpreferred conformations on the UK132 peptide backbone. As a result, UK132 cyclised with TBMM or TBME is not able to adopt a conformation that is complementary to the surface of huPA, ultimately impeding the formation of optimal inter-molecular non-covalent interactions needed for binding to huPA. Another reason could be that in solution the different bicyclic peptides have preferred folds that differ from those in their bound conformations. Moreover, we cannot exclude that the mesitylene linker of peptide UK132–TBMB forms direct contacts with huPA and that these interactions are perturbed with the introduction of methyl or ethyl chains.

Further studies involving the use of monocyclic and bicyclic peptide analogues in which the second loop of UK132 or UK140 has been either removed or substituted with one not evolved *in vitro* have allowed us to better appreciate its contribution in binding. For instance, replacement of the affinity matured second peptide loop with a flexible glycine-serine linker yielded a bicyclic peptide inhibitor with >150-fold lower potency. This suggests that both UK132 peptide loops might contribute to huPA binding, a strategy used by other high affinity and good target specificity bicycle peptide inhibitors previously reported.[25] However, inhibition studies using monocyclic peptide analogues of UK132 and UK140 revealed that of the two loops, the first one plays a major contribution in inhibiting huPA. Though the first loop appears to have a predominant role in blocking the catalytic activity of the enzyme, the contribution of the second loop in binding is not to be underestimated. Indeed, the inhibitory potency of monocyclic peptides derived solely from the first peptide loop of UK132 and UK140 is still 6- and 22-fold weaker than that of the same bicyclic peptides, respectively. One possible explanation is that side-chain and/or main-chain atoms of the second loop might provide a network of noncovalent intra-molecular interactions with side-chain and/or main-chain atoms of the first loop, ultimately affecting its conformation and binding to huPA. This might also better explain why bicyclic peptide UK132 modified with small organic linkers TBMM and TBME showed lower inhibitory potency than UK132-TBMB. Indeed, we cannot exclude that the additional methyl or ethyl chains present in TBMM and TBME, respectively, might have altered the network of noncovalent intra-molecular interactions between the different peptide loops otherwise existing in UK132 modified with TBMB. It's worth to notice that among bicycle peptides isolated during the affinity maturation process, some showed a >10-fold lower inhibitory potency than UK132 despite having an identical first peptide loop. Furthermore, although both bicyclic peptides UK132 and UK140 have an identical second loop, and UK140 ($K_i$ = 0.20 μM) is ~2-fold more potent than UK132 ($K_i$ = 0.33 μM), the macrocyclic ring of UK140 ($K_i$ = 4.58 μM), bearing a lysine instead of an arginine in position 5, is approximately 3-fold less potent than that of UK132 ($K_i$ = 2.18 μM). Moreover, we cannot rule out that the same side-chain and/or main-chain atoms of the second loop can themselves establish direct inter-molecular contacts with residues of huPA, ultimately leading to higher binding affinity. Given that monocyclic analogues of the second loop of both UK132 and UK140 did not inhibit huPA, we can speculate that these interactions might involve residues present in non-catalytic and less conserved subsites of huPA, such as S1′, S2, S3. Taken together these data support an intimate cooperation of both peptide loops in binding huPA. While the first loop appears to have a predominant and direct role in blocking the catalytic activity of the enzyme, the contribution of the second loop cannot be overlooked.

In conclusion, our research efforts led to the development of UK140, a novel bicyclic peptide inhibitor of huPA that is 10-fold more potent than the best parental clone and can cross-react with the orthologue

muPA. Even though UK140 can weakly inhibit the paralogue human trypsin, its ability to block both huPA and orthologue muPA with $K_i$ values in the low micromolar range, it offers the opportunity to generate a human and murine cross-reactive bicycle peptide inhibitor that can be tested in mouse model ultimately allowing not only the evaluation of its therapeutic efficacy but also a better assessment of treatment toxicity, as well as simpler and lower cost clinical trials, by facilitating the transition from pre-clinical mouse models to clinical studies in humans. Further studies, including the use of non-canonical amino acids and peptidomimetic approaches, will be oriented toward the development of bicycle peptide variants with higher potency and retained cross-reactivity toward huPA and muPA. While many challenges remain, the ability to evolve bicyclic peptide inhibitors that combine key qualities of protein inhibitors such as the high affinity and specificity with advantages of small molecules such as the small size and potentially good extravasation properties, provide novel and attractive strategies for the development of potent and specific anti-metastatic therapies.

## 4. Material and methods

### 4.1. Recombinant production of the catalytic domain of huPA

The low molecular weight huPA (LMW huPA-N145Q) comprising the truncated 23 amino acid peptide fragment of chain A (Lys136-Lys158 in huPA numbering) and the catalytic domain of huPA (also termed chain B; Ile159-Leu411 in huPA numbering or Ile16-Leu250 in chymotrypsin numbering), mutated in one position to eliminate the glycosylation site (Asn145Gln), was expressed by transient transfection of suspension-adapted human embryonic kidney FreeStyle 293-F cells (HEK-293-F) as previously described.[24] Briefly, 1 mg of pSecTagA-LMW-huPA-N145Q plasmid encoding LMW huPA-N145Q protein was premixed to linear polyethylenimine (PEI, Polysciences, Heppenheim, Germany) and Opti-MEM (Thermo Fisher Scientific, Dreieich, Germany) and used to transfect 1 L of high cell density ($1 \times 10^6$ cells/mL) HEK-293-F cells growing in serum-free FreeStyle™ 293 Expression Medium (Thermo Fisher Scientific, Dreieich, Germany) in an orbitally shaken one-liter flask at 180 rpm in a Forma Steri-Cycle 370 $CO_2$ incubator (Thermo Fisher Scientific, Dreieich, Germany) at 37°C in the presence of 5% $CO_2$.[55,56] At the end of the 7-day phase production, cells were harvested by centrifugation at 5500 rpm for 20 min at 4 °C on an Avanti J-25 centrifuge (Backman Coulter, Indianapolis, USA). Any additional cell debris was removed from the medium by filtration through 0.45 μm low protein binding membranes (Prat-dumas, Bourg, France).

### 4.2. Purification of the catalytic domain of huPA

The recombinant LMW huPA-N145Q was purified as previously described.[24] Briefly, the recombinant huPA was concentrated by using 10000 MWCO Amicon Ultra ultrafiltration tube (Merck Novagen, Nottingham, UK) at 3000 g and 4 °C on a 5810R centrifuge (Eppendorf, Hamburg, Germany) and diluted five-fold with Buffer A (50 mM sodium phosphate pH 6.2). The recombinant huPA was captured on 10 mL strong cation exchange SP sepharose fast flow resin (Cytiva, Freiburg, Germany) packed on a XK-16 gravity column (Cytiva, Freiburg, Germany) pre-equilibrated with Buffer B (25 mM sodium phosphate pH 6.4). The diluted medium was passed through the pre-equilibrated resin at 4 °C. After extensive washing with Buffer B (25 mM sodium phosphate pH 6.4), recombinant huPA was eluted with Buffer C (25 mM sodium phosphate, 500 mM NaCl, pH 6.4). The huPA containing fractions were pooled, concentrated by using 10000 MWCO Amicon Ultra ultrafiltration tube (Merck Novagen, Nottingham, UK) at 3000 g and 4 °C on an 5810R centrifuge (Eppendorf, Hamburg, Germany), diluted ten-fold with Buffer A (50 mM sodium phosphate pH 6.2), and subjected to second cation exchange HiScreen SP HP pre-packed chromatography column (Cytiva, Freiburg, Germany) connected to an AKTA purifier system (Cytiva, Freiburg, Germany). The diluted protein was passed through the resin pre-equilibrated with Buffer B at a flow rate of 1.0 mL/min at 4 °C. After extensive washing with Buffer B, recombinant huPA was eluted with Buffer C by applying a linear NaCl gradient (0 – 500 mM). The eluted protein showed a single band in SDS-PAGE, with an apparent molecular mass of about 32 kDa. Afterwards, the recombinant huPA was converted into its active two-chain form by plasmin cleavage. To a solution of 150 μM LMW-huPA-N145Q in Buffer D (50 mM HEPES, 150 mM NaCl, pH 8.0), 200 nM human plasmin (HPLM, Haematologic Technologies, Essex, VT, USA) was added (ratio 500:1). After incubation for 4 h at room-temperature, the cleaved activated protein was further purified by size exclusion chromatography using a HiLoad 26/60 Superdex 200 prep-grade column (Cytiva, Freiburg, Germany) and Buffer E (50 mM HEPES, 100 mM NaCl, pH 7.0) on an AKTA purifier system (Cytiva, Freiburg, Germany). The protein was eluted as a monomer giving a single band in SDS-PAGE confirming the complete cleavage, with a molecular mass of about 28 kDa under reducing conditions. The pure and activated recombinant huPA in Buffer E was then concentrated to 10 mg/mL (347 μM) by using 5000 MWCO PES Vivaspin-20 ultrafiltration tube (Sartorius-Stedim Biotech GmbH, Göttingen, Germany) at 3000 g and 4 °C on 5810R centrifuge (Eppendorf, Hamburg, Germany). The activity of recombinant huPA before and after plasmin activation was assessed by incubating the protein with the fluorogenic substrate Z-Gly-Gly-Arg-AMC (50 μM; Bachem, Bubendorf, Switzerland) in 10 mM Tris-Cl, pH 7.4, 150 mM NaCl, 10 mM $MgCl_2$, 1 mM $CaCl_2$, 0.1% w/v BSA, 0.01% v/v Triton-X100 buffer. The initial velocities were monitored as changes in fluorescence intensity during 30 min on a Spectramax Gemini fluorescence plate reader (excitation at 355 nm, emission recording at 460 nm; Molecular Devices, Sunnyvale, CA, USA). No inhibitors were added in the buffers.

### 4.3. Chemical biotinylation of huPA

Reactive EZ-link sulfo-NHS-LC-biotin (Pierce, Rockford, IL, USA) was dissolved in pure anhydrous DMSO to obtain a final concentration of 10 mM. Protein conjugate containing biotin was prepared by incubating recombinant huPA, at concentration of 10 μM in 100 mM sodium phosphate, 150 mM NaCl, pH 7.4, with twenty-fold molar excess of EZ-link sulfo-NHS-LC-biotin (200 μM) for 1 h at room temperature. Excess of unreacted or hydrolysed biotinylation reagent was removed by gel filtration with a PD-10 column (Cytiva, Freiburg, Germany) equilibrated with buffer 50 mM NaAc, 200 mM NaCl, pH 5.5. Fractions corresponding to the expected protein peak were pulled and concentrated to a final concentration of 1 mg/mL using 10000 MWCO Vivaspin-20 ultrafiltration tube (Sartorius-Stedim Biotech GmbH, Göttingen, Germany) at 4000 g and 4 °C on a Heraeus Multifuge 3L-R centrifuge (Thermo Fisher Scientific, Dreieich, Germany). Final protein concentration was determined spectrophotometrically at 280 nm (GeneQuant 100, GE Healthcare, Uppsala, Sweden). The molecular mass of recombinant LMW huPA-N145Q before and after chemical biotinylation was determined with electrospray ionization mass spectrometry (ESI − MS) performed on a quadrupole time-of-flight mass spectrometer (Q − TOF) Ultima API (Waters, Millford, MA, USA) operated with the standard ESI source and in positive ionisation mode.[55] Recombinant LMW huPA-N145Q protein were desalted by performing multiple consecutive dilutions with sterile $H_2O$ mQ followed by concentration using YM-10 (10000 MWCO Regenerated Cellulose, Microcon, Millipore) at 4000 g and 4 °C on a Heraeus Multifuge 3L-R centrifuge (Thermo Fisher Scientific, Dreieich, Germany). The ESI-Q-TOF mass spectrometer was calibrated for a range of 500 to 2500 *m/z*. Ten microliter desalted protein samples (5 μM) were injected for each measurement. Data were acquired, processed, and analysed using the software MassLynx v 4.1 (Waters). The ability of the biotinylated recombinant huPA to bind to streptavidin was verified by incubating the protein with magnetic streptavidin beads and analysing the bound and unbound protein fraction by SDS-PAGE.

### 4.4. Cloning of the affinity maturation phage library

The affinity maturation phage library was designed with the format $ACN^{A}/_{S}R^{F}/^{S}_{Y}/_{T}GCXXXXXXCG$ (X = random amino acid). DNA sequence encoding the semi-random peptide library and the linker glycine-glycine-serine-glycine (GGSG) was appended to the gene encoding the mutated (Ile101Thr) disulfide-free domains D1 and D2 of phage protein 3 (fdg3p0ss21-I101T) in a PCR reaction using the reverse primer sfi2-notfo (5′-CCATGGCCCCCGAGGCCGCGGCCGCATTGACAGG-3′) and the forward degenerate primer sficxale3 (5′-TATGCGGCCCAGCCGGC-CATGGCAGCATGCAACKCNCGCT-WYWCNGGCTGCNNKNNKNNKNNKNNKNNKTGTGGCGGTTCTGGCG-CTG-3′ (Microsynth AG, Balgach, Switzerland). The presence of codon "KCN" ensures a 50% probability of inserting either a serine or an alanine in this position. Similarly, the usage of codons "TWY" and "WCN" guarantees similar frequency of amino acids phenylalanine or tyrosine and serine or threonine in that specific position, respectively. The PCR products were digested with *Sfi*I and cloned into the pEco2 phage vector previously linearised using the same restriction enzymes. A 16 h ligation was performed by applying a temperature gradient ranging from 12 °C to 16 °C. Electroporation of the ligation product (10 μg) into *E. coli* TG1 cells yielded $2 \times 10^8$ colony forming units (c.f.u.) on large (140 mm diameter) chloramphenicol (30 μg/mL) 2YT agar plates. Colonies were scraped off the plates with 2YT media, supplemented with 15% v/v glycerol and stored at −80 °C.

### 4.5. Phage selection of affinity-matured bicyclic peptides

Two liters of 2YT/chloramphenicol (30 μg/ml) medium were inoculated with cells from the affinity maturation library glycerol stocks to obtain an $OD_{600}$ of 0.1. The culture was shaken (200 rpm) for 4 h at 37 °C and another 12 h at 30 °C. The phage particles were purified by PEG precipitation as previously described.[33] PEG purified phage particles ($10^{12}$ t.u.) were reduced in 20 mL of 20 mM $NH_4HCO_3$, pH 8.0 with 1 mM TCEP at 42 °C for 1 h. The concentration of TCEP was subsequently reduced by repetitive concentration and dilution steps with reaction buffer (20 mM $NH_4HCO_3$, 5 mM EDTA, pH 8.0, degassed) in a Vivaspin-20 filter (MWCO of 10000, Sartorius-Stedim Biotech GmbH, Göttingen, Germany). The volume of the phage solution was adjusted to 32 mL with reaction buffer and 8 mL of 50 μM TBMB in 100% v/v acetonitrile (ACN) were added to obtain a final TBMB concentration of 10 μM. The reaction was incubated at 30 °C for 1 h before non-reacted TBMB was removed by precipitation of the phage with 1/5 vol of 20% w/v PEG6000, 2.5 M NaCl on ice and centrifugation at 4000 g for 30 min. The precipitated chemically modified phage particles (typically $10^{10}$-$10^{11}$ t.u.) were then dissolved in 3 mL washing buffer (10 mM Tris-Cl, pH 7.4, 150 mM NaCl, 10 mM $MgCl_2$, 1 mM $CaCl_2$) and blocked by addition of 1.5 mL of washing buffer containing 3% w/v BSA and 0.3% v/v Tween 20 for 30 min with rotation (10 rpm). At the same time the biotinylated LMW huPA-N145Q (10 μg) and the streptavidin magnetic beads (50 μL; Dynabeads M-280 Streptavidin from Invitrogen, Paisley, UK) were also individually blocked in 0.5 mL washing buffer (10 mM Tris-Cl, pH 7.4, 150 mM NaCl, 10 mM $MgCl_2$, 1 mM $CaCl_2$) containing 1% w/v BSA and 0.1% v/v Tween 20 for 30 min at room temperature with rotation (10 rpm). The blocked biotinylated recombinant huPA (0.5 mL) and streptavidin magnetic beads (0.5 mL) were then mixed and incubated for other 10 min at room temperature with rotation (10 rpm). The biotinylated recombinant huPA immobilised on streptavidin magnetic beads was washed six times with washing buffer containing 1% w/v BSA and 0.1% v/v Tween 20. The biotinylated recombinant huPA immobilised on streptavidin magnetic beads (1 mL) and the blocked phage particles (4.5 mL) were mixed and incubated for 1 h on a rotating wheel (10 rpm) at room temperature. The beads were washed eight times with washing buffer containing 0.1% v/v Tween 20 and twice with washing buffer. The phage particles were eluted by incubation with 100 μL of 50 mM glycine, pH 2.2 for 5 min. Eluted phage particles were transferred to 50 μL of 1 M Tris-Cl, pH 8 for neutralisation and incubated with 50 mL TG1 cells at $OD_{600} = 0.4$ for 90 min in a static incubator at 37 °C. Cells were pelleted by centrifugation at 4000 g for 5 min, resuspended in 2 mL 2YT and plated on large 2YT/chloramphenicol (30 μg/mL) plates. A second round of panning was performed following the same procedure but using neutravidin-coated magnetic beads instead of streptavidin in order to prevent the enrichment of streptavidin-specific peptides. To minimise undesired avidity effects and enhance the stringency of the selection, we deviated from our previous "direct capture" selection strategy and performed an "indirect capture" selection strategy (also known as the "solution binding" approach).[57] In this strategy, the chemically modified phage particles were initially mixed with the biotinylated recombinant huPA in homogeneous solution and the phage-target complexes were next incubated with the neutravidin-coated magnetic beads in order to capture those phage particles whose displayed bicyclic peptides bound the biotinylated recombinant huPA during the initial step. Notably, this two-step capture approach enables precise fine-tuning of the target concentration and allows the kinetics of the binding reaction to be better controlled.[57] Neutravidin beads were prepared by reacting 1.5 mg neutravidin (Pierce, Rockford, IL, USA) dissolved in 100 mM borate buffer pH 9.5 with 1 mL tosylactivated magnetic beads ($2 \times 10^9$ beads/mL; Dynabeads M−280 Tosylactivated, Invitrogen Dynal Biotech AS, Oslo, Norway) according to the supplier's instructions. In this second round of affinity selection 20-fold less biotinylated recombinant huPA (0.5 μg) was used and further blocked in 0.5 mL of washing buffer (10 mM Tris-Cl, pH 7.4, 150 mM NaCl, 10 mM $MgCl_2$, 1 mM $CaCl_2$) containing 1% w/v BSA and 0.1% v/v Tween 20 for 30 min at room temperature with rotation (10 rpm). At the same time, the chemically modified phage particles dissolved in 3 mL washing buffer were blocked by addition of 1.5 mL of washing buffer containing 3% w/v BSA and 0.3% v/v Tween 20 for 30 min. Blocked biotinylated recombinant huPA (0.5 mL) and phage particles (4.5 mL) were mixed and incubated for additional 30 min on a rotating wheel (10 rpm) at room temperature. Next 50 μL of neutravidin magnetic beads, blocked in 0.5 mL of washing buffer containing 1% w/v BSA and 0.1% v/v Tween 20 for 30 min, were added to the phage/huPA mixture and incubated for 5 min at room temperature with rotation (10 rpm). The phage binders were then eluted at acidic pH and allowed to infect and propagate in TG1 cells. Finally, to promote the selection of clones with increased binding affinity for huPA we allowed the phage particles to evolve through a third round of "indirect capture" equilibrium-based selection using even lower amounts of biotinylated huPA (0.05 ug) and by replacing neutravidin beads with streptavidin beads.

### 4.6. Cloning of bicyclic peptide-D1-D2 fusion proteins

The genes that encode the peptides isolated in the phage affinity maturation process were cloned into pETALX vector for cytoplasmic expression of bicyclic peptide-D1-D2 fusion proteins. The pETALX vector, is a modified version of pET28b (Merck Novagen, Nottingham, UK), and enables direct subcloning of gene encoding peptide fusion proteins from the phage plasmid while preserving unaltered the functional *N*-terminus region of the peptide, otherwise modified by the addition of an extra alanine when using the commercially available pET28b plasmid. Constructs for cytoplasmic expression were generated using the following strategy. Briefly, bacterial colonies raised from *E. coli* cells infected with selected phage particles were scraped from the plates and the mixture of phage plasmids isolated with a Qiagen miniprep kit (Qiagen GmbH, Hilden, Germany). Phage plasmids were then digested with *Not*I-HF and *Sph*I-HF (New England Biolabs, Ipswich, USA) restriction enzymes, the selected peptides fused to the disulfide-free domains D1 and D2 of g3p gel purified and further ligated into pETALX expression vector previously linearised using the same restriction enzymes and dephosphorylated using FastAP thermosensitive alkaline phosphatase (Fermentas GmbH, Leon-Rot, Germany). *E. coli* XL-1 blue competent cells were transformed with the ligation product, plated on

2YT/kanamycin (50 μg/mL kanamycin) plates and each DNA-encoding peptide sequence revealed by Sanger sequencing (Macrogen, Seoul, South Korea).

### 4.7. Recombinant production and purification of bicyclic peptide-D1-D2 fusion proteins

Peptide-D1-D2-$His_6$ fusion proteins were expressed and purified as follows. Half liter of 2YT/kanamycin (50 μg/mL) cultures were inoculated with *over-night* cultures of transformed *E.coli* BL21-CodonPlus-RIL cells (1:100 dilution) and incubated in a shaker (250 rpm) at 37 °C. Protein expression was induced by addition of 1 mM isopropyl-$\beta$-D-1-thiogalactopyranoside (IPTG) at an $OD_{600}$ of 0.6–0.8 and the cultures were shaken for 12 h at 25 °C. Cells were harvested by centrifugation at 8000 g for 20 min and resuspended in 20 mL lysis buffer (30 mM $Na_2HPO_4/NaH_2PO_4$, pH 7.4, 300 mM NaCl, 1 mM TCEP, 0.1% v/v Triton X-100, 100 μg/mL lysozyme, 50 μg/mL DNase). Cells were additionally lysed by sonication and spun for 25 min at 10000 g. The clarified supernatants were purified sequentially by Ni-affinity chromatography and gel filtration using an automated AKTAxpress FPLC system (Cytiva, Freiburg, Germany) which allowed the purification of four peptide-D1-D2 fusion proteins in parallel. In the Ni-affinity chromatography step the lysates were loaded onto 1 mL HisTrap FF columns (GE Healthcare, Uppsala, Sweden) that were equilibrated with buffer A (30 mM $Na_2HPO_4/NaH_2PO_4$, pH 7.4, 300 mM NaCl, 10 mM imidazole, 1 mM TCEP, degassed). The columns were washed with buffer A and the proteins eluted in a single peak at 200–400 mM imidazole by applying a linear gradient (20–100%) of buffer B (30 mM $Na_2HPO_4/NaH_2PO_4$, pH 7.4, 300 mM NaCl, 500 mM imidazole, 1 mM TCEP, degassed). In the subsequent size exclusion chromatography step the proteins were purified using a HiPrep 16/60 Sephacryl S-100 HR column (Cytiva, Freiburg, Germany) and reaction buffer with TCEP (20 mM $NH_4HCO_3$, 5 mM EDTA, 1 μM TCEP, pH 8.0, degassed). All fusion proteins were eluted as a monomer giving a single band in SDS-PAGE, with an apparent molecular mass of about 28 kDa and a final yield of 5–20 mg/L of cell culture. Due to the treatment with TCEP during cell lysis and protein purification, the cysteines in the final product were reduced.

### 4.8. Cyclisation of peptide-D1-D2 fusion proteins with TBMB

The peptide appendix was cyclised by mixing 0.5 mL TBMB (500 μM) in 100% v/v ACN with 4.5 mL of reduced peptide-D1-D2 (10 μM) in reaction buffer (20 mM $NH_4HCO_3$, 5 mM EDTA, pH 8.0, degassed) at 30 °C for 1 h. Non-reacted TBMB was removed by size exclusion chromatography with a PD-10 column (GE Healthcare, Uppsala, Sweden) equilibrated with washing buffer (10 mM Tris-Cl, pH 7.4, 150 mM NaCl, 10 mM $MgCl_2$, 1 mM $CaCl_2$). The concentration of peptide-D1-D2 conjugates was determined by measuring the optical absorption at 280 nm (GeneQuant 100, GE Healthcare, Uppsala, Sweden).

### 4.9. Mass spectrometric analysis of peptide-D1-D2 fusion proteins

The molecular mass of peptide-D1-D2 fusion proteins, before and after chemical modification with TBMB, was determined with electrospray ionisation mass spectrometry (ESI–MS) performed on a quadrupole time-of-flight mass spectrometer (Q–TOF) Ultima API (Waters, Millford, MA, USA) operated with the standard ESI source and in the positive ionisation mode. Both unmodified (15–100 μM in 20 mM $NH_4HCO_3$, 5 mM EDTA, pH 8.0 and 1 μM TCEP buffer) and modified (5–10 μM in 10 mM Tris-Cl, pH 7.4, 150 mM NaCl, 10 mM $MgCl_2$, 1 mM $CaCl_2$) fusion protein samples were desalted either by gel filtration using a PD-10 column (GE Healthcare, Uppsala, Sweden) equilibrated with $H_2O$ mQ or by analytical reversed-phase high performance liquid chromatography (RP-HPLC) on a Waters HPLC system equipped with Waters 2487 dual λ absorbance detector and with both Waters 600 pump and controller (Waters, Millford, MA, USA) and a Vydac C4 (214TP) column (5 μm, 4.6 × 250 mm) (Grace & Co., USA). At a flow rate of 1 mL/min, a linear gradient was applied with a mobile phase composed of eluant A (0.1% v/v aqueous trifluoroacetic acid (TFA) solution, 99.9% v/v $H_2O$) and eluant B (99.9% v/v ACN and 0.1% v/v TFA). The purified peptide-D1-D2 fusion proteins were freeze-dried and dissolved in $H_2O$ mQ. For mass spectrometric analysis, the samples were mixed with 50% v/v ACN, 49.9% v/v $H_2O$, 0.1% v/v formic acid. Data were acquired, processed, and analysed using the software MassLynx™ version 4.1 (Waters, Millford, MA, USA).

### 4.10. Determination of inhibition constants ($K_i$s) of cyclic peptide-D1-D2 fusion proteins

The inhibition constants $K_i$s were determined by incubating different concentrations of the TBMB-conjugated peptide fusion proteins (two-fold dilutions: 0.0117, 0.0234, 0.0469, 0.0938, 0.1875, 0.375, 0.75, 1.5, 3, 6 and 12 μM for the selected affinity maturated clones) with fixed concentration of recombinant huPA (4 nM). The enzymatic assays were performed at 25 °C using the fluorogenic substrate Z-Gly-Gly-Arg-AMC (50 μM; Bachem, Bubendorf, Switzerland) in 10 mM Tris-Cl, pH 7.4, 150 mM NaCl, 10 mM $MgCl_2$, 1 mM $CaCl_2$, 0.1% w/v BSA, 0.01% v/v Triton-X100 buffer. The initial velocities were monitored as changes in fluorescence intensity during 30 min on a Spectramax Gemini fluorescence plate reader (excitation at 355 nm, emission recording at 460 nm; Molecular Devices, Sunnyvale, CA, USA). Apparent equilibrium constants $K_i^{app}$ values were determined by non-linear regression analyses of $V_i/V_0$ versus $[I]_0$ using Eq. (1):

$$V_i/V_0 = 1 - \frac{[E]_0 + [I]_0 + K_i^{app} - \sqrt{\left([E]_0 + [I]_0 + K_i^{app}\right)^2 - 4[E]_0[I]_0}}{2[E]_0} \quad (1)$$

where $V_i$ and $V_0$ are the reaction velocities in the presence and absence of inhibitor, respectively. $[E]_0$ and $[I]_0$ represent the total enzyme and inhibitor concentration, respectively. $K_i^{app}$ is the apparent inhibition constant in the presence of fluorogenic substrate. The final $K_i$ was subsequently determined by correcting for the competitive effect of the substrate $[S]_0$ using Eq. (2):

$$K_i = K_i^{app}/\left(1 + [S]_0/K_m\right) \quad (2)$$

where $K_m$ is the Michaelis constant for the hydrolysis of Z-Gly-Gly-Arg-AMC catalysed by huPA which has been determined by standard Michaelis-Menten equations as described below. Values were determined using either OriginPro 8G software (OriginLab Corporation, Northamppton, MA, USA) or GraphPad Prism 8.0.0. software (GraphPad software, Inc., San Diego, California).

### 4.11. Determination of binding constant ($K_D$s) using surface plasmon resonance (SPR)

The equilibrium binding constant ($K_D$), association rate constant ("on rate", $k_{on}$) and dissociation rate constant ("off rate", $k_{off}$) for the interaction of UK113-D1-D2, UK115 -D1-D2 and UK132-D1-D2 fusion proteins with huPA were determined by surface plasmon resonance (SPR) using a Biacore 3000 instrument (GE Healthcare, Uppsala, Sweden). Biotinylated huPA was immobilised on a streptavidin-coated chip (Sensor chip SA; GE Healthcare, Uppsala, Sweden) by injecting the protein (1 μg/mL) dissolved in 50 mM NaAc, 200 mM NaCl, pH 5.5 buffer at a continuous flow rate of 10 μL/min a capture of 1500 RU per flow cell was reached (where RU is the response unit and 1 RU = 1 pg of protein per $mm^2$). Binding experiments were performed in running buffer (10 mM Tris-Cl pH 7.4, 150 mM NaCl, 10 mM $MgCl_2$, 1 mM $CaCl_2$) at a continuous flow rate of 10 μL/min and 25 °C. Unbound biotinylated huPA was removed by injecting 100 μL glycine pH 2.8 at 50 μL/min for 12 s. For the determination of the dissociation constants, the monomeric fraction of UK113-D1-D2, UK115-D1-D2 and UK132-D1-D2 fusion

proteins were collected by size-exclusion chromatography as described above. Serial 25 μL injections of two-fold dilution of the monomers (0.375, 0.750, 1.5, 3, 6, 12 and 24 μM), were applied through the sensor surface for 180 s under a continuous flow rate of 10 μL/min. After 180 s of dissociation time, the sensor surface was regenerated for the next sample using a 10 μL pulse of glycine pH 2.8 at 50 μL/min. In all experiments an untreated streptavidin flow cell without huPA protein was used as reference to correct binding response for bulk refractive index changes and unspecific binding. The association rate constant ($k_{on}$) and the dissociation rate constant ($k_{off}$) were determined by global fitting mode. Data were fitted to a Langmuir binding model assuming stoichiometric (1:1) interactions by using BIAevaluation software version 4.1 (Biacore). The equilibrium binding constant ($K_D$) values were calculated as the ratio of $k_{off}$ to $k_{on}$ ($K_D = k_{off}/k_{on}$). The $K_D$ were also determined by plotting binding responses in the steady-state region of the sensograms ($R_{eq}$) versus analyte peptide-D1-D2 concentration (C). The data were subjected to non-linear regression fitting according to the following Eq. (3):

$$R_{eq} = \frac{R_{max} C}{C + K_D} \quad (3)$$

where $R_{max}$ is the maximum binding response in RU, and $K_D$ is the dissociation constant. The data were analysed by using either OriginPro 8G software (OriginLab Corporation) or GraphPad Prism 8.0.0. software (GraphPad software, Inc.).

### 4.12. Chemical synthesis of bicyclic peptides

Peptides with a free amine at the *N*-terminus and an amide at the C-terminus were chemically synthetised by standard Fmoc (9-fluorenylmethoxycarbonyl) solid-phase peptide synthesis (SPPS). Fmoc-protected amino acids were purchased either from Iris biotech GmbH (Marktredwitz, Germany) or from Novabiochem (Darmstadt, Germany). Fmoc-rink amide AM resin (100–200 mesh mesh, loading 0.26 mmol/g resin) and Fmoc-rink amide MBHA resin (100–200 mesh, loading 0.4–0.9 mmol/g resin) were purchased from Iris biotech GmbH (Marktredwitz, Germany) and Novabiochem (Darmstadt, Germany), respectively. Chemicals O-Benzotriazole-N,N,N',N'-tetramethyl-uroniumhexafluoro-phosphate (HBTU, ChemPep, Wellington, FL, USA), (Benzotriazol-1-yloxy)tripyrrolidinophosphonium hexafluorophosphate (PyBOP, Novabiochem, Darmstadt, Germany) N,*N*-Diisopropylethylamine (DIPEA, Merck Schuchardt OHG, Hohenbrunn, Germany), acetic anhydride (Novabiochem, Darmstadt, Germany), formic acid (Sigma-Aldrich, Darmstadt, Germany), trifluoroacetic acid (TFA, Sigma-Aldrich, Darmstadt, Germany or Chemie GmbH, Steinheim, Germany), 1,2-ethanedithiol (EDT, Fluka Chemie GmbH, Buchs, Switzerland), octanedithiol (ODT, Sigma-Aldrich, Darmstadt, Germany), thioanisole (Fluka Chemie GmbH, Buchs, Switzerland), anisole (Novabiochem, Darmstadt, Germany), piperidine (Fluka, Machelen, Belgium or Sigma-Aldrich, Darmstadt, Germany), phenol (Acros Organics, Geel, Belgium), dichloromethane (DCM, Novabiochem, Darmstadt, Germany), N,*N*-dimethylformamide (DMF, Novabiochem, Darmstadt, Germany), *N*-methylmorpholine (NMM, Sigma-Aldrich, Darmstadt, Germany), *N*-methylpirrolidone (NMP, VWR, Pennsylvania, USA), acetonitrile (ACN, Sigma-Aldrich, Darmstadt, Germany), 1,3,5-tris(bromomethyl)benzene (TBMB, Sigma-Aldrich, Darmstadt, Germany), 1,3-bis(bromomethyl) benzene (DBMB, Sigma-Aldrich, Darmstadt, Germany), 2,4,6-*tris*-(bromomethyl)-mesitylene (TBMM, Sigma-Aldrich, Darmstadt, Germany) and 1,3,5-*tris*-(bromethyl)-2,4,6-triethyl-benzol (TBME, Sigma-Aldrich, Darmstadt, Germany) were used as received without further purification. Peptides were chemically synthesised using either the Advanced ChemTech 348 Ω automated peptide synthesiser (aapptec, Louisville, USA) or the ResPepSLi automated peptide synthesiser (Intavis Bioanalytical Instruments, Köln, Germany). In the case of Advanced ChemTech 348 Ω automated peptide synthesiser, a Rink Amide AM resin (0.03 mmol scale) was used. Coupling step was carried out twice for each amino acids (6 eq., 0.4 M solution in DMF) using the HBTU (5.5 eq, 0.4 M solution in DMF)-DIPEA (9 eq, 1.2 M solution in DMF) coupling system. Fmoc groups were removed using a 20% (v/v) solution of piperidine in DMF (2.5 mL × 2). The final peptides were deprotected (side-chain protected groups) and cleaved from the resin using a TFA/thioanisole/$H_2O$ /phenol/EDT mixture (90/2.5/2.5/2.5/2.5%v/v, 4 mL) for 3 h at room temperature. The resin was removed by filtration under vacuum and the peptides were precipitated with cold diethyl ether (40 mL). The precipitated peptides were resuspended and washed with diethyl ether (20 mL × 2). Finally, the peptides were dissolved in $H_2O$:ACN (5:2) and lyophilized. In the case of ResPepSLi automated peptide synthesiser, a Rink Amide MBHA resin (0.01 mmol scale) was used. Fmoc groups were removed using a 20% v/v solution of piperidine in DMF (180 μL × 2). Amino acid coupling was carried out twice for each Fmoc-amino acid (7.5 eq., 0.5 M solution in DMF) using the PyBOP/NMM coupling system (5.5 eq. 0.4 M / 9 eq. 4 M in DMF). Fmoc groups were removed using a 20% v/v solution of piperidine in DMF. Final acetylation capping was performed using a 5% v/v solution of acetic anhydride in DMF. DCM washes (0.3 mL × 5) were performed at the end of the synthetic process. NMP was used as cosolvent in the peptide synthesis. A 4 M NMM solution in DMF was added as weak base for Fmoc deprotection. The final peptides were deprotected (side-chain protected groups) and cleaved from the resin using a TFA/thioanisole/$H_2O$/anisole/ODT mixture (90/2.5/2.5/2.5/2.5% v/v) for 3 h at room temperature. The resin was removed by filtration under vacuum and the peptides were precipitated with cold diethyl ether (50 mL). The precipitated peptides were resuspended in diethyl ether (30 mL × 2) and centrifuged (3 times). Finally, the peptides were dissolved in $H_2O$:ACN (1:1), freeze-dried and lyophilised on a LIO-5PDGT (5Pascal).

### 4.13. Chemical cyclisation of peptides

Bicyclic peptides UK113, UK115, UK132, UK137, UK138, UK139, UK140, UK141, UK142 and UK18 + UK132 modified with TBMB were obtained by reacting crude peptides (1 mM) in 5% v/v DMSO, 65% v/v 20 mM $NH_4HCO_3$, pH 8.0 and 30% v/v ACN with TBMB (2 mM) for 1 h at 30 °C. Monocyclic peptide UK132$^{CSC}$ modified with DBMB was obtained by reacting crude peptide (0.5 mM) in 5% v/v DMSO, 45% v/v 20 mM $NH_4HCO_3$, pH 8.0 and 50% v/v ACN with DBMB (1 mM) for 2 h at 30 °C. Bicyclic peptide UK132 modified with TBMM was obtained by reacting crude peptide (0.5 mM) in 5% v/v DMSO, 20% v/v 20 mM $NH_4HCO_3$, pH 8.0 and 75% v/v ACN with TBMM (1 mM) for 2 h at 30 °C. Bicyclic peptide UK132 modified with TBME was obtained by reacting crude peptide (0.5 mM) in 5% v/v DMSO, 20% v/v 20 mM $NH_4HCO_3$, pH 8.0 and 75% v/v ACN with TBME (1 mM) for 2 h at 30 °C. Monocyclic peptide L1 UK140, L2 UK132, L1 UK132 and L2 UK115 modified with DBMB were obtained by reacting crude peptides (1 mM) in 70% v/v 20 mM $NH_4HCO_3$, pH 8.0 and 30% v/v ACN with DBMB (2 mM) for 1 h at 30 °C. The reaction products were purified by preparative reversed-phase high performance liquid chromatography (RP-HPLC) using either a Vydac C18 (218TP) column (22 × 250 mm) (Grace & Co., USA) or a C18 SymmetryPrep functionalized silica column (7 μm, 19 mm × 150 mm) (Waters, Millford, MA, USA) connected to a Waters Delta Prep LC 4000 System equipped with a Waters 2489 dual λ absorbance detector, a Waters 600 pump and a PrepLC Controller (Waters, Millford, MA, USA). A flow rate of 20 mL/min and a linear gradient (10% to 50% in 35 min) with a mobile phase composed of eluant A (99.9% v/v $H_2O$, 0.1% v/v TFA) and eluant B (99.9% v/v ACN and 0.1% v/v TFA) was applied. The purified peptides were freeze-dried. The purity and molecular mass of the peptides was assessed by LC-ESI as described below. Concentrations of peptides were determined using BioPhotometer D30 UV spectrophotometry (Eppendorf, Hamburg, Germany).

### 4.14. Mass spectrometric analysis of synthetic peptides

The molecular mass of synthetic peptides was determined either with an Axima-CFR plus MALDI-TOF mass spectrometer (Axima-CFR plus, Kratos Shimadzu Biotech, Manchester, UK) or by electrospray ionisation mass spectrometry (ESI–MS) performed on a single quadrupole liquid chromatograph InfinityLab LC/MSD mass spectrometer coupled to a 1260 Infinity II LC system (Agilent Technologies, Santa Clara, CA, USA). For the MALDI-TOF analysis, peptide samples (0.1–100 μM in 0.1% v/v TFA/10–30% v/v ACN in $H_2O$) were mixed 1:1 with a solution of matrix, 10 mg/mL α-cyano-4-hydroxycinnamic acid (α-CHCA) in 50% v/v ACN, 49.9% v/v $H_2O$, 0.1% v/v TFA and loaded onto a MALDI carrier plate for mass determination. For the ESI-MS analysis, peptide samples were mixed with 50% v/v ACN, 50% v/v $H_2O$. Peptides were run at a flow rate of 1 mL/min with a linear gradient of solvent B over 15 min (solvent A: 99.9% v/v $H_2O$ and 0.1% v/v formic acid; solvent B: 99.9% v/v ACN and 0.1% v/v formic acid). The reversed-phase HPLC column was a Nucleosil 100–5 C18 (5 μm, 125 mm × 4 mm; Macherey-Nagel, Dueren, Germany). The system operated with the standard ESI source and in the positive ionisation mode. Data were acquired, processed and analysed using the Agilent OpenLAB CDS (Agilent Technologies, Santa Clara, CA, USA) and MestReNova (Mestrelab Research, Santiago de Compostela, Spain).

### 4.15. Activity determination of chemically synthesised inhibitors

Residual activities were measured in 150 μL volume of buffer containing 10 mM Tris-Cl, pH 7.4, 150 mM NaCl, 10 mM $MgCl_2$, 1 mM $CaCl_2$, 0.1% w/v BSA, 0.01% v/v Triton-X100 and 5% v/v DMSO. Final concentration of huPA enzyme was 1.5 nM in all the experiments. Concentrations of tested peptides were ranging from a maximum of 10 mM to a minimum of 5 nM. Two-fold dilutions were prepared for each tested peptide. The measurements were performed on a Spectramax Gemini fluorescence plate reader (Molecular Devices, Sunnyvale, CA, USA) or on a Tecan microplate reader (Tecan infinite 200 pro, Tecan Trading AG, Switzerland). The enzymatic reactions were performed at 25 °C for 30 min, under shaking with an excitation wavelength of 355 nm and an emission recording at 460 nm. The initial velocities were monitored as changes in fluorescence intensity. Apparent equilibrium constant $K_i^{apps}$ values were determined by non-linear regression analyses of $V_i/V_0$ versus $[I]_0$ using Eq. (1). The final $K_i$s were subsequently determined by correcting for the competitive effect of the substrate $[S]_0$ using Eq. (2). The kinetic constant $K_m$ for the hydrolysis of fluorogenic substrate catalysed by huPA was determined by standard Michaelis-Menten equations as described above. Values were determined using either OriginPro 8G software (OriginLab Corporation, Northamppton, MA, USA) or GraphPad Prism 8.0.0. software (GraphPad software, Inc., San Diego, California).

### 4.16. Specificity determination of chemically synthesised bicyclic peptide inhibitors

Residual activities were measured in 150 μL volume of buffer containing 10 mM Tris-Cl, pH 7.4, 150 mM NaCl, 10 mM $MgCl_2$, 1 mM $CaCl_2$, 0.1% w/v BSA, 0.01% v/v Triton-X100 and 5% v/v DMSO. Final concentrations of serine proteases were the following: human uPA (UPA-LMW, from human urine, 33 kDa; Molecular Innovations, Novi, MI, USA) 1.5 nM, mouse uPA (MUPA-LMW, recombinantly produced in insect cells, 31 kDa; Molecular Innovations, Novi, MI, USA) 12 nM, human tPA (HTPATC, recombinant, 70 kDa; Molecular Innovations, Novi, MI, USA) 7.5 nM, mouse tPA (MTPA, recombinantly produced in insect cells, 70 kDa; Molecular Innovations, Novi, MI, USA) 6 nM, human trypsin (HTRYP, from human pancreas, 25 kDa; Molecular Innovations, Novi, MI, USA) 0.05 nM, human plasmin (HPLM, from human plasma, 85 kDa; Molecular Innovations, Novi, MI, USA) 1.5 nM, human plasma kallikrein (IHPKA, from human plasma, 86 kDa; Innovative Research, Novi, MI, USA) 0.5 nM, human thrombin (IHT, from human plasma, 37 kDa, Innovative Research, Novi, MI, USA) 10 nM, human factor XIIa (IHFXIIa, from human plasma, 80 kDa; Innovative Research, Novi, MI, USA) 6 nM, human factor Xa (HCXA-0060, Haematologic Technologies, Essex, VT, USA) 1 nM, human factor XIa (HCXIA-0160, Haematologic Technologies, Essex, VT, USA) 10 nM, human factor VIIa (HCVIIA-0031, Haematologic Technologies, Essex, VT, USA) 100 nM and human activated protein C (HCAPC-0080, Haematologic Technologies, Essex, VT, USA) 10 nM. Two-fold dilutions of UK132 bicyclic peptide inhibitor were prepared ranging from 12 mM to 300 nM for all the proteases. For human uPA an extra two-fold UK132 inhibitor dilution experiment was performed by using inhibitor concentrations ranging from 300 nM to 3 nM. For the determination of the $K_i$ inhibitory constants, the following fluorogenic substrates were used at final concentration of 50 μM: Z-Gly-Gly-Arg-AMC (for human uPA, murine uPA, human tPA, murine tPA, human trypsin, human thrombin and human factor XIIa; Bachem, Bubendorf, Switzerland), Z-Phe-Arg-AMC (for human plasma kallikrein; Bachem, Bubendorf, Switzerland), H-D-Val-Leu-Lys-AMC (for human plasmin; Bachem, Bubendorf, Switzerland). A final concentration of 200 μM was instead used for the chromogenic substrates Z-D-Arg-Gly-Arg-pNA (for human factor Xa; Cromogenix DiaPharma,West Chester, OH), pyroGlu-Pro-Arg-pNA (for human factor XIa and aPC, Cromogenix DiaPharma,West Chester, OH) and $CH_3SO_2$-D-Cha-But-Arg-pNA (for human factor VIIa, Merck Novagen, Nottingham, UK). For the huPA, muPA, htPA, mtPA, human trypsin, human plasmin, human plasma kallikrein, human thrombin and human factor XIIa, the enzymatic reactions were performed at 25 °C. The initial velocities were monitored as changes in fluorescence intensity during 30 min on a Spectramax Gemini fluorescence plate reader (excitation at 355 nm, emission recording at 460 nm; Molecular Devices, Sunnyvale, CA, USA). For human factor VIIa, Xa, XIa and human activated protein C the enzymatic reactions were performed at 25 °C. The initial velocities were monitored as changes in chromogenic intensity during 1 h (human factor Xa and human activated protein C) or 3 hrs (human factor VIIa and XIa) on a Tecan Infinite 200 Pro microplate reader (absorbance at 405 nm; Tecan Trading AG, Switzerland). Apparent equilibrium constants $K_i^{apps}$ values were determined by non-linear regression analyses of $V_i/V_0$ versus $[I]_0$ using Eq. (1). The final $K_i$s were subsequently determined by correcting for the competitive effect of the substrate $[S]_0$ using Eq. (2). The kinetic constants $K_m$s for the hydrolysis of fluorogenic substrate, catalysed by each protease, were determined by standard Michaelis-Menten equations as described above. Values were determined using either OriginPro 8G software (OriginLab Corporation, Northamppton, MA, USA) or GraphPad Prism 8.0.0. software (GraphPad software, Inc., San Diego, California).

## Funding

This work was supported by the Ministerio de Educacion España (post-doc fellowship EX2009-0730 to J.M.S.).

## Declaration of Competing Interest

The authors declare that they have no known competing financial interests or personal relationships that could have appeared to influence the work reported in this paper.

## Data availability

Data will be made available on request.

## Acknowledgments

The authors would like to thank Prof. Christian Heinis for his valuable input and constant support. We thank Dr. Laure Menin for assistance with mass spectrometry experiments and analysis and Chiara

Cescon for assistance with peptide synthesis. We are grateful to all the group members for helpful discussions and for critical reading of the manuscript.

## Appendix A. Supplementary material

Supplementary data to this article can be found online at https://doi.org/10.1016/j.bmc.2023.117499.

## References


1] Chapin JC, Hajjar KA. Fibrinolysis and the control of blood coagulation. *Blood Rev*. 2015;29:17–24. https://doi.org/10.1016/j.blre.2014.09.003.
2 Alfano D, Franco P, Vocca I, et al. The urokinase plasminogen activator and its receptor. Role in cell growth and apoptosis. *Thrombosis Haemostasis*. 2005;93(2): 205–211. https://doi.org/10.1160/TH04-09-0592.
3 Mahmood N, Mihalcioiu C, Rabbani SA. Multifaceted role of the urokinase-type plasminogen activator (uPA) and its receptor (uPAR): Diagnostic, prognostic, and therapeutic applications. *Front Oncol*. 2018;8. https://doi.org/10.3389/fonc.2018.00024.
4 Wyganowska-Świątkowska M, Tarnowski M, Murtagh D, Skrzypczak-Jankun E, Jankun J. Proteolysis is the most fundamental property of malignancy and its inhibition may be used therapeutically. *Int J Mol Med*. 2019;43:15–25. https://doi.org/10.3892/ijmm.2018.3983.
5 Kuş C, Özer E, Korkmaz Y, Yurtcu E, Dağalp R. Novel Inhibitors of Urokinase-type Plasminogen Activators: 4-(3H-imidazo[4,5-b]pyridin-2-yl)-N-Substituted Benzamide and Benzamidine Compound. *Mini-Rev Med Chem*. 2018;18:1753–1758. https://doi.org/10.2174/1389557518666180816110740.
6 Oldenberg E, Schar CR, Lange EL, et al. Abstract B055: New potential therapeutic applications of WX-UK1 as a specific and potent inhibitor of human trypsin-2 and human trypsin-3. *Mol Cancer Ther*. 2018;17:B055–B. https://doi.org/10.1158/1535-7163.targ-17-b055.
7 Froriep D, Clement B, Bittner F, et al. Activation of the anti-cancer agent upamostat by the mARC enzyme system. *Xenobiotica*. 2013;43:780–784. https://doi.org/10.3109/00498254.2013.767481.
8 Heinemann V, Ebert MP, Laubender RP, Bevan P, Mala C, Boeck S. Phase II randomised proof-of-concept study of the urokinase inhibitor upamostat (WX-671) in combination with gemcitabine compared with gemcitabine alone in patients with non-resectable, locally advanced pancreatic cancer. *Br J Cancer*. 2013;108:766–770. https://doi.org/10.1038/bjc.2013.62.
9 Masucci MT, Minopoli M, Di Carluccio G, Motti ML, Carriero MV. Therapeutic Strategies Targeting Urokinase and Its Receptor in Cancer. *Cancers*. 2022;14(3). https://doi.org/10.3390/cancers14030498.
10 Rudzińska M, Daglioglu C, Savvateeva LV, Kaci FN, Antoine R, Zamyatnin AA. Current status and perspectives of protease inhibitors and their combination with nanosized drug delivery systems for targeted cancer therapy. *Drug Des Devel Ther*. 2021;15:9–20. https://doi.org/10.2147/DDDT.S285852.
11 Goldstein LJ. Experience in phase I trials and an upcoming phase II study with uPA inhibitors in metastatic breast cancer. *Breast Care*. 2008;3:25–28. https://doi.org/10.1159/000151733.
12 Heinemann V, Ebert MP, Pinter T, Bevan P, Neville NG, Mala C. Randomized phase II trial with an uPA inhibitor (WX-671) in patients with locally advanced nonmetastatic pancreatic cancer. *J Clin Oncol*. 2010;28:4060. https://doi.org/10.1200/jco.2010.28.15_suppl.4060.
13 Setyono-Han B, Stürzebecher J, Schmalix WA, et al. Suppression of rat breast cancer metastasis and reduction of primary tumour growth by the small synthetic urokinase inhibitor WX-UKI. *Thromb Haemost*. 2005;93:779–786. https://doi.org/10.1160/TH04-11-0712.
14 Oldenburg E, Schar RC, et al. Abstract 4200: New potential therapeutic applications of WX-UK1, as a specific and potent inhibitor of human trypsin-like protease. https://doi.org/10.1158/1538-7445.AM2018-4200.
15 Stefan Sperl M, M, Buergle M, W, Schmalix G; K, Wosikowski P; B, Clement K. Hydroxyamidine and hydroxyguandine compounds as urolinase inhibitors. Patent *No. US20060142305A1* 2009;2(12).
16 Zorzi A, Deyle K, Heinis C. Cyclic peptide therapeutics: past, present and future. *Curr Opin Chem Biol*. 2017;38:24–29. https://doi.org/10.1016/j.cbpa.2017.02.006.
17 Wang L, Wang N, Zhang W, et al. Therapeutic peptides: current applications and future directions. *Signal Transduction Targeted Therapy*. 2022;7(1). https://doi.org/10.1038/s41392-022-00904-4.
18 Xu P, Andreasen PA, Huang M. Structural principles in the development of cyclic peptidic enzyme inhibitors. *Int J Biol Sci*. 2017;13:1222–1233. https://doi.org/10.7150/ijbs.21597.
19 Xu P, Huang M. Small Peptides as Modulators of Serine Proteases. *Curr Med Chem*. 2018;27:3686–3705. https://doi.org/10.2174/0929867325666181016163630.
20 Schweinitz A, Steinmetzer T, Banke IJ, et al. Design of novel and selective inhibitors of urokinase-type plasminogen activator with improved pharmacokinetic properties for use as antimetastatic agents. *J Biol Chem*. 2004;279:33613–33622. https://doi.org/10.1074/jbc.M314151200.
21 Wendt MD, Geyer A, McClellan WJ, et al. Interaction with the S1β-pocket of urokinase: 8-heterocycle substituted and 6,8-disubstituted 2-naphthamidine urokinase inhibitors. *Bioorg Med Chem Lett*. 2004;14:3063–3068. https://doi.org/10.1016/j.bmcl.2004.04.030.
22 Wendt MD, Rockway TW, Geyer A, et al. Identification of Novel Binding Interactions in the Development of Potent, Selective 2-Naphthamidine Inhibitors of Urokinase. Synthesis, Structural Analysis, and SAR of N-Phenyl Amide 6-Substitution. *J Med Chem*. 2004;47(2):303–324. https://doi.org/10.1021/jm0300072.
23 Henneke I, Greschus S, Savai R, et al. Inhibition of urokinase activity reduces primary tumor growth and metastasis formation in a murine lung carcinoma model. *Am J Respir Crit Care Med*. 2010;181:611–619. https://doi.org/10.1164/rccm.200903-0342OC.
24 Angelini A, Cendron L, Chen S, et al. Bicyclic peptide inhibitor reveals large contact interface with a protease target. *ACS Chem Biol*. 2012;7:817–821. https://doi.org/10.1021/cb200478t.
25 Deyle K, Kong XD, Heinis C. Phage Selection of Cyclic Peptides for Application in Research and Drug Development. *Acc Chem Res*. 2017;50:1866–1874. https://doi.org/10.1021/acs.accounts.7b00184.
26 Angelini A, Morales-Sanfrutos J, Diderich P, Chen S, Heinis C. Bicyclization and tethering to albumin yields long-acting peptide antagonists. *J Med Chem*. 2012;55: 10187–10197. https://doi.org/10.1021/jm301276e.
27 Räder AFB, Weinmüller M, Reichart F, et al. Orally Active Peptides: Is There a Magic Bullet? *Angewandte Chemie - International Edition*. 2018;57:14414–14438. https://doi.org/10.1002/anie.201807298.
28 Hansen M, Wind T, Blouse GE, et al. A urokinase-type plasminogen activator-inhibiting cyclic peptide with an unusual P2 residue and an extended protease binding surface demonstrates new modalities for enzyme inhibition. *J Biol Chem*. 2005;280:38424–38437. https://doi.org/10.1074/jbc.M505933200.
29 Zhao G, Yuan C, Wind T, Huang Z, Andreasen PA, Huang M. Structural basis of specificity of a peptidyl urokinase inhibitor, upain-1. *J Struct Biol*. 2007;160:1–10. https://doi.org/10.1016/j.jsb.2007.06.003.
30 Jiang L, Svane ASP, Sørensen HP, et al. The binding mechanism of a peptidic cyclic serine protease inhibitor. *J Mol Biol*. 2011;412:235–250. https://doi.org/10.1016/j.jmb.2011.07.028.
31 Andersen LM, Wind T, Hansen HD, Andreasen PA. A cyclic peptidylic inhibitor of murine urokinase-type plasminogen activator: Changing species specificity by substitution of a single residue. *Biochem J*. 2008;412:447–457. https://doi.org/10.1042/BJ20071646.
32 Wang D, Yang Y, Jiang L, et al. Suppression of Tumor Growth and Metastases by Targeted Intervention in Urokinase Activity with Cyclic Peptides. *J Med Chem*. 2019; 62:2172–2183. https://doi.org/10.1021/acs.jmedchem.8b01908.
33 Heinis C, Rutherford T, Freund S, Winter G. Phage-encoded combinatorial chemical libraries based on bicyclic peptides. *Nat Chem Biol*. 2009;5:502–507. https://doi.org/10.1038/nchembio.184.
34 Chen S, Rentero Rebollo I, Buth SA, et al. Bicyclic peptide ligands pulled out of cysteine-rich peptide libraries. *J Am Chem Soc*. 2013;135:6562–6569. https://doi.org/10.1021/ja400461h.
35 Chen S, Bertoldo D, Angelini A, Pojer F, Heinis C. Peptide ligands stabilized by small molecules. *Angewandte Chemie - International Edition*. 2014;53:1602–1606. https://doi.org/10.1002/anie.201309459.
36 Rebollo IR, Sabisz M, Baeriswyl V, Heinis C. Identification of target-binding peptide motifs by high-throughput sequencing of phage-selected peptides. *Nucl Acids Res*. 2014;42(22). https://doi.org/10.1093/nar/gku940.
37 Rebollo IR, Angelini A, Heinis C. Phage display libraries of differently sized bicyclic peptides. *MedChemComm*. 2013;4:145–150. https://doi.org/10.1039/c2md20171b.
38 Chen S, Gfeller D, Buth SA, Michielin O, Leiman PG, Heinis C. Improving binding affinity and stability of peptide ligands by substituting glycines with D-amino acids. *Chembiochem*. 2013;14:1316–1322. https://doi.org/10.1002/cbic.201300228.
39 Pollaro L, Raghunathan S, Morales-Sanfrutos J, Angelini A, Kontos S, Heinis C. Bicyclic peptides conjugated to an albumin-binding tag diffuse efficiently into solid tumors. *Mol Cancer Ther*. 2015;14:151–161. https://doi.org/10.1158/1535-7163.MCT-14-0534.
40 Tagirasa R, Yoo E. Role of Serine Proteases at the Tumor-Stroma Interface. *Front Immunol*. 2022;13:1–12. https://doi.org/10.3389/fimmu.2022.832418.
41 Shih-Chi Su, Chiao-Wen Lin, Wei-En Yang. The urokinase-type plasminogen activator (uPA) system as a biomarker and therapeutic target in human malignancies. Expert Opin Therap Targets. Published online 2015:1–16. doi:10.1517/14728222.2016.1113260.
42 Mackman RL, Katz BA, Breitenbucher JG, et al. Exploiting subsite S1 of trypsin-like serine proteases for selectivity: Potent and selective inhibitors of urokinase-type plasminogen activator. *J Med Chem*. 2001;44:3856–3871. https://doi.org/10.1021/jm010244+.
43 Michael Laskowski J, Kato I. Protein inhibitors of proteinases. *Nature*. 1969;223:426. https://doi.org/10.1038/223426b0.
44 Lin Z, Jiang L, Yuan C, et al. Structural basis for recognition of urokinase-type plasminogen activator by plasminogen activator inhibitor-1. *J Biol Chem*. 2011;286: 7027–7032. https://doi.org/10.1074/jbc.M110.204537.
45 Jendroszek A, Madsen JB, Chana-Muñoz A, et al. Biochemical and structural analyses suggest that plasminogen activators coevolved with their cognate protein substrates and inhibitors. *J Biol Chem*. 2019;294:3794–3805. https://doi.org/10.1074/jbc.RA118.005419.
46 Mishra M. Evolutionary Aspects of the Structural Convergence and Functional Diversification of Kunitz-Domain Inhibitors. *J Mol Evol*. 2020;88:537–548. https://doi.org/10.1007/s00239-020-09959-9.
47 Zhou HX. Loops, Linkages, Rings, Catenanes, Cages, and Crowders: Entropy-Based Strategies for Stabilizing Proteins. *Acc Chem Res*. 2004;37:123–130. https://doi.org/10.1021/ar0302282.
48 Suárez D, Díaz N. Ligand Strain and Entropic Effects on the Binding of Macrocyclic and Linear Inhibitors: Molecular Modeling of Penicillopepsin Complexes. *J Chem Inf Model*. 2017;57:2045–2055. https://doi.org/10.1021/acs.jcim.7b00355.

49 Boehr DD, Nussinov R, Wright PE. The role of dynamic conformational ensembles in biomolecular recognition. *Nat Chem Biol*. 2009;5:789–796. https://doi.org/10.1038/nchembio.232.

50 Wang CK, Swedberg JE, Northfield SE, Craik DJ. Effects of Cyclization on Peptide Backbone Dynamics. *J Phys Chem B*. 2015;119:15821–15830. https://doi.org/10.1021/acs.jpcb.5b11085.

51 Udugamasooriya DG, Spaller MR. Conformational constraint in protein ligand design and the inconsistency of binding entropy. *Biopolymers*. 2008;89:653–667. https://doi.org/10.1002/bip.20983.

52 Gaucher JF, Reille-Seroussi M, Broussy S. Structural and ITC Characterization of Peptide-Protein Binding: Thermodynamic Consequences of Cyclization Constraints, a Case Study on Vascular Endothelial Growth Factor Ligands. *Chem - A Eur J*. 2022;28 (48). https://doi.org/10.1002/chem.202200465.

53 Roodbeen R, Paaske B, Jiang L, et al. Bicyclic peptide inhibitor of urokinase-type plasminogen activator: Mode of action. *Chembiochem*. 2013;14:2179–2188. https://doi.org/10.1002/cbic.201300335.

54 Fox JM, Zhao M, Fink MJ, Kang K, Whitesides GM. The Molecular Origin of Enthalpy/Entropy Compensation in Biomolecular Recognition. *Annu Rev Biophys*. 2018;47:223–250. https://doi.org/10.1146/annurev-biophys-070816-033743.

55 Angelini A, Diderich P, Morales-Sanfrutos J, et al. Chemical macrocyclization of peptides fused to antibody Fc fragments. *Bioconjug Chem*. 2012;23:1856–1863. https://doi.org/10.1021/bc300184m.

56 Angelini A, Miyabe Y, Newsted D, et al. Directed evolution of broadly crossreactive chemokine-blocking antibodies efficacious in arthritis. *Nat Commun*. 2018;9(1). https://doi.org/10.1038/s41467-018-03687-x.

57 Smith GP, Petrenko VA. Phage display. *Chem Rev*. 1997;901:391–410. https://doi.org/10.1021/cr960065d.